Article

Cell Host & Microbe

Accelerated Aging and Clearance of Host Anti-inflammatory Enzymes by Discrete Pathogens Fuels Sepsis

Graphical Abstract

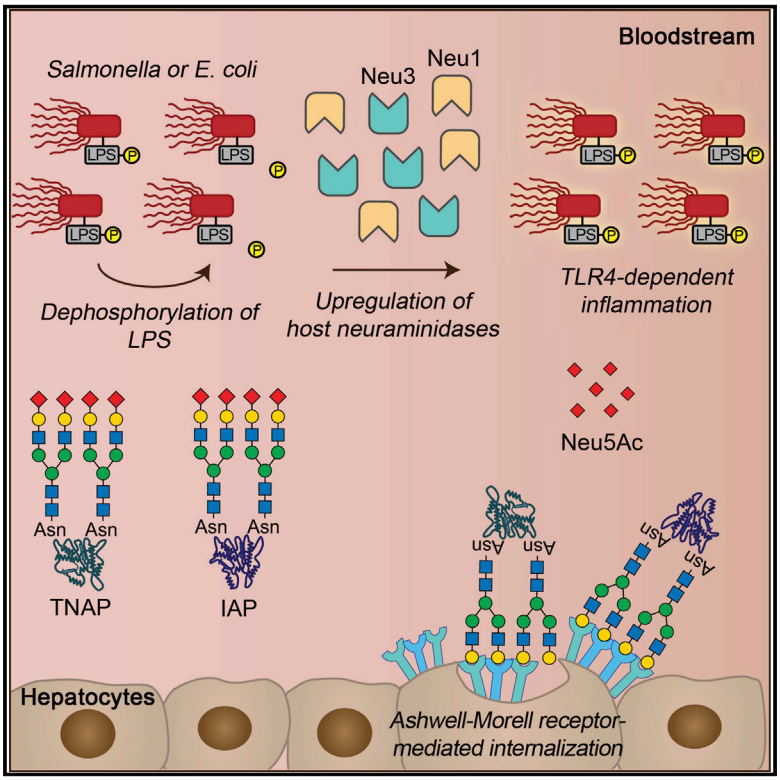

Highlights

- The pathophysiology of sepsis can be stratified by pathogens and host responses
- Host neuraminidases induced by LPS activation of TLR4 accelerate AP aging and clearance mechanisms
- The Ashwell-Morell receptor and ST3Gal6 antagonistically participate in AP homeostasis
- Neuraminidase inhibition and AP augmentation therapeutically diminish TLR4 downstream pathology

Authors

Won Ho Yang, Douglas M. Heithoff, Peter V. Aziz, ..., Victor Nizet, Michael J. Mahan, Jamey D. Marth

Correspondence

jmarth@sbpdiscovery.org

In Brief

Yang et al. develop a comparative protocol to identify mechanisms in the pathogenesis of experimental sepsis. Discrete Gram-negative pathogens elicit a TLR4-dependent host response that disrupts the homeostatic regulation of alkaline phosphatase (AP) isozymes through neuraminidase activation. AP augmentation and neuraminidase inhibition are therapeutic by maintaining the de-toxification of LPS-phosphate.

Yang et al., 2018, Cell Host & Microbe *24*, 500–513
October 10, 2018
https://doi.org/10.1016/j.chom.2018.09.011

CellPress

CellPress

Cell Host & Microbe
Article

Accelerated Aging and Clearance of Host Anti-inflammatory Enzymes by Discrete Pathogens Fuels Sepsis

Won Ho Yang,[1,2] Douglas M. Heithoff,[1,3] Peter V. Aziz,[1,2,3] Benjamin Haslund-Gourley,[1,2,3] Julia S. Westman,[1,2] Sonoko Narisawa,[2] Anthony B. Pinkerton,[2] José Luis Millán,[2] Victor Nizet,[4,5] Michael J. Mahan,[1,3] and Jamey D. Marth[1,2,3,6,*]

[1]Center for Nanomedicine, University of California Santa Barbara, Santa Barbara, California 93106, USA
[2]Sanford-Burham-Prebys Medical Discovery Institute, University of California Santa Barbara, Santa Barbara, California 93106, USA
[3]Department of Molecular, Cellular, and Developmental Biology, University of California Santa Barbara, Santa Barbara, California 93106, USA
[4]Department of Pediatrics, University of California San Diego, La Jolla, CA 92093
[5]Skaggs School of Pharmacy and Pharmaceutical Sciences, University of California San Diego, La Jolla, CA 92093, USA
[6]Lead Contact
*Correspondence: jmarth@sbpdiscovery.org
https://doi.org/10.1016/j.chom.2018.09.011

SUMMARY

Sepsis is a life-threatening inflammatory syndrome accompanying a bloodstream infection. Frequently secondary to pathogenic bacterial infections, sepsis remains difficult to treat as a singular disease mechanism. We compared the pathogenesis of murine sepsis experimentally elicited by five bacterial pathogens and report similarities among host responses to Gram-negative *Salmonella* and *E. coli*. We observed that a host protective mechanism involving de-toxification of lipopolysaccharide by circulating alkaline phosphatase (AP) isozymes was incapacitated during sepsis caused by *Salmonella* or *E. coli* through activation of host Toll-like receptor 4, which triggered Neu1 and Neu3 neuraminidase induction. Elevated neuraminidase activity accelerated the molecular aging and clearance of AP isozymes, thereby intensifying disease. Mice deficient in the sialyltransferase ST3Gal6 displayed increased disease severity, while deficiency of the endocytic lectin hepatic Ashwell-Morell receptor was protective. AP augmentation or neuraminidase inhibition diminished inflammation and promoted host survival. This study illuminates distinct routes of sepsis pathogenesis, which may inform therapeutic development.

INTRODUCTION

Sepsis is a life-threatening bloodstream infection accompanied by pathological inflammation and organ system dysfunction. The leading cause of death in non-cardiac intensive care units, sepsis is increasing in incidence, while no new effective therapies have been developed in decades (Fleischmann et al., 2016; Gaieski et al., 2013; Marshall, 2014; Orban et al., 2017; Stevenson et al., 2014). Among patients with severe sepsis or septic shock, mortality averages 25%, with many survivors experiencing long-term disabilities from tissue and organ damage caused by thrombosis, hypoperfusion, and hyperinflammation (Chang et al., 2010; Hawiger and Musser, 2011; Iwashyna et al., 2010; Stevenson et al., 2014). The development of more effective treatments for sepsis likely requires additional knowledge of host responses and pathogenic mechanisms activated at earlier stages of disease onset.

At later disease stages, sepsis can appear as a stereotypical disease process of uncontrolled inflammation and coagulopathy. Several identified host factors and cytokines drive inflammatory tissue and vascular injury, but their targeting has yet to lead to safe and effective therapies (Chaudhry et al., 2013; D'Elia et al., 2013; Schulte et al., 2013). Sentinel events in the pathogenesis of human sepsis are not easily identified, as diverse patient groups are infected at unknown times by pathogens that sometimes evade clinical detection. Gram-positive bacterial pathogens commonly identified in sepsis patients include *Staphylococcus aureus* (*SA*) and *Streptococcus pneumoniae* (*SPN*), while sepsis due to Gram-negative bacterial pathogens such as *Escherichia coli* (*EC*) and *Salmonella spp.* has increased in recent years, accompanied by worrisome antibiotic resistance (Hartman et al., 2013; Vincent et al., 2009).

We developed a protocol for comparative studies of experimental sepsis in mice at early and later disease stages calibrated by specific post-infection times and blood pathogen colony-forming unit (*cfu*) thresholds. This approach provided a reproducible data platform from which cross-comparisons were made using multiple Gram-positive and Gram-negative bacterial pathogens and different routes of infection. Our analysis revealed a common mechanism of host protection unique to the Gram-negative infections studied, involving the regulated half-lives of circulating enzymes capable of detoxifying bacterial lipopolysaccharide (LPS). However, this host-protective mechanism stands at risk of pathogen subversion resulting in severe inflammation and increased mortality in established sepsis. Efforts to bolster this protective mechanism reduced disease pathophysiology and mortality, suggesting a pharmacological target in a subset of infections to counteract the pathogenesis of sepsis at its early stages.

RESULTS

Acquired and Selective Deficiency of Alkaline Phosphatase in the Pathogenesis of Murine Sepsis

Experimental analysis of bacterial sepsis was undertaken in the murine model, where genomic signatures of inflammatory responses were recently shown to closely correlate to those of humans (Takao and Miyakawa, 2015). Although cecal ligation and puncture (CLP) is the most frequently used experimental sepsis model, we chose not to use CLP for multiple reasons. CLP generates polymicrobial infections, which represent a small subset of human sepsis cases—typically much less than 10% among populations surveyed (Lin et al., 2010; Pammi et al., 2014). CLP can also generate variable results depending on ligation length, quantity, and quality of intestinal perforations as well as different numbers of Gram-negative and Gram-positive bacteria released from the lumen of the intestine (Dejager et al., 2011; Singleton and Wischmeyer, 2003). Sepsis resulting from CLP can evolve to become either Gram-positive or Gram-negative, while the precise identification and titers of the pathogens involved are rarely possible to obtain and monitor. We therefore compared host response patterns and disease outcomes separately among five different bacterial pathogen isolates identified from invasive human infections. These included two common Gram-negative bacterial pathogens, *EC* and *Salmonella enterica* Typhimurium (*ST*), and two pre-eminent Gram-positive bacterial pathogens, *SPN* and *SA*; for the latter, both methicillin-sensitive (*MSSA*) and methicillin-resistant (*MRSA*) strains were tested. For all bacterial strains, disease severity and mortality were directly proportional to increased bacterial *cf.*u in the bloodstream. We thus applied criteria for data inclusion in comparative sepsis pathophysiology analyses involving attainment of minimum and maximum thresholds of blood *cf*u at specified times post-infection.

Sepsis caused by the Gram-negative bacterial pathogens *EC* and *ST* was linked to an unexpected reduction of alkaline phosphatase (AP) activity measured at approximately 50% of normal by blood chemistry analyses. This reduction was associated with similarly decreased abundance of both tissue-nonspecific alkaline phosphatase (TNAP) and intestinal alkaline phosphatase (IAP) (Figures 1A–1D). TNAP has been found to control bone mineralization, and IAP functions in fat absorption through the intestinal epithelium as well as in protection against colitis (Narisawa et al., 1997, 2003; Parlato et al., 2018; Yang et al., 2017). TNAP is produced by a variety of cell types, including those in bone, liver, and kidney, while IAP is secreted exclusively by enterocytes of the small intestine (Millán, 2006). Alkaline phosphatase isozymes further include placental alkaline phosphatase (PLAP) and germ cell alkaline phosphatase (GCLP) in human and embryonic alkaline phosphatase (EAP) in mouse (Millán, 2006); however, these other isozymes are not found in the blood stream and were not analyzed in our studies. In contrast to sepsis caused by *EC* or *ST* pathogens, there was no change to blood AP activity and AP isozyme abundance in sepsis resulting from infections of Gram-positive *Streptococcal* or *Staphylococcal* bacterial pathogens *SPN* or *MRSA* (Figures 1E–1H) as well as the related *Staphylococcal* isolate *MSSA* (Figures S1A and S1B).

The impact of reduced AP levels in the host during sepsis caused by *EC* or *ST* infections was probed by intravenous (i.v.) pharmacological restoration of AP activity using calf IAP (cIAP). AP activity is known to de-toxify the Gram-negative bacterial endotoxin lipopolysaccharide (LPS) through de-phosphorylation of the lipid A moiety (Bates et al., 2007; Beumer et al., 2003; Koyama et al., 2002; Poelstra et al., 1997; Tuin et al., 2006). The toxic form of LPS contains two phosphate groups coupled to glucosamines; removal of a single phosphate group by AP activity is sufficient to generate a monophosphoryl lipid A that is 100-fold less toxic than fully phosphorylated LPS (Bentala et al., 2002; Park et al., 2009; Schromm et al., 1998). Both TNAP and IAP can de-phosphorylate and de-toxify LPS (Pettengill et al., 2017); however, the specific phosphate(s) hydrolyzed are not currently defined. We measured LPS-phosphate levels using the malachite green phosphate assay and compared findings to total LPS in the contexts of AP reduction and cIAP treatment. Our findings revealed that decreased LPS-phosphate was linked to increased AP activity provided by either endogenous or exogenous sources (Figures 1I–1L). cIAP administration further reduced blood inflammatory cytokine levels and markedly improved mouse survival following infection with the *EC* and *ST* pathogens (Figures 1M–1P). In contrast, cIAP treatment did not alter inflammatory cytokine expression or frequencies of mortality during sepsis caused by Gram-positive *SPN*, *MRSA*, or *MSSA* pathogens (Figures 1Q–1V and S1C–S1E). The reduction of AP activity was not dependent upon the route of infection, as *ST* infection elicited by direct intraperitoneal (i.p.) infection resulted in a more rapid disease course than orogastric challenge while yielding similar but earlier reductions of AP levels requiring more rapid cIAP replacement therapy (Figures S1F–S1K).

Accelerated Molecular Aging of AP Isozymes and Clearance by the Ashwell-Morell Receptor

Given the importance of AP abundance and activity in protecting the host during sepsis caused by Gram-negative *EC* and *ST* pathogens, we sought to identify the mechanism(s) governing TNAP and IAP regulation. Reductions of TNAP and IAP protein abundance occurred without diminished mRNA levels in tissues known to produce these isozymes (Figures S2A and S2B). Rather, the half-lives of both TNAP and IAP in blood circulation were significantly reduced (Figures 2A and 2B). By contrast, TNAP and IAP half-lives were unaltered in sepsis caused by *SPN* and *MRSA* (Figures 2C and 2D), consistent with retention of normal AP activity. TNAP and IAP are glycoprotein enzymes synthesized in the secretory pathway of cells and glycosylated prior to secretion (Millán, 2006). Sepsis caused by *EC* and *ST* reduced MAL-II lectin binding to a subset of total sialic acids, coincident with increased exposure of underlying galactose linkages recognized by ECA and RCA lectins (Figures 2E and 2F). No changes involving a subset of α2-6-linked sialic acids or core 1 *O*-glycan sialylation were detected using the SNA and PNA lectins, respectively. Neither TNAP nor IAP underwent similar glycan remodeling during sepsis caused by *SPN* or *MRSA* (Figures S2C and S2D) with retention of normal AP isozyme half-lives and abundance.

We suspected that one or more host endocytic lectin receptor(s), likely to include the hepatic Ashwell-Morell receptor

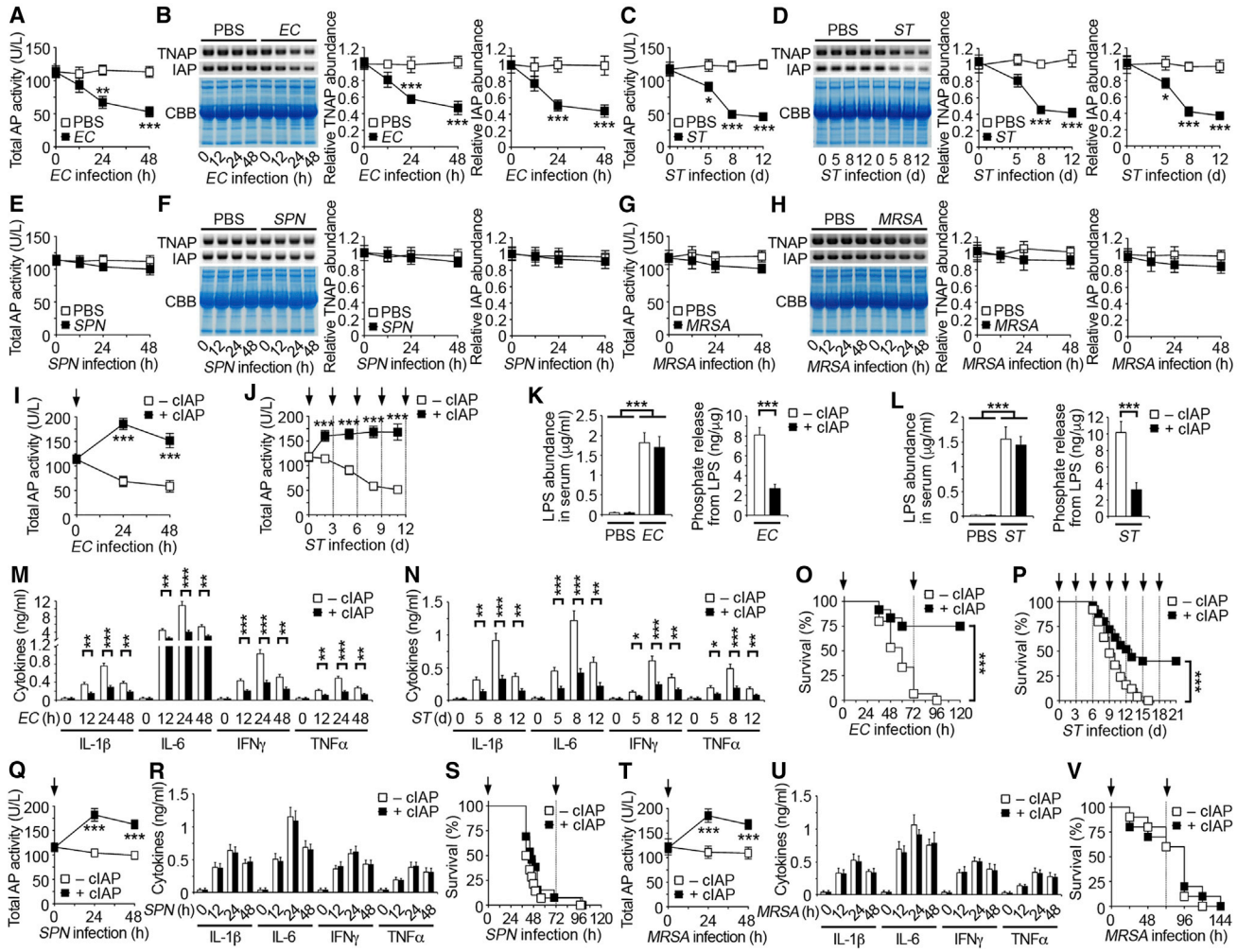

Figure 1. Pathogen-Selective Reduction of Host Anti-inflammatory Alkaline Phosphatase

(A, C, E, and G) Total alkaline phosphatase (AP) activity measured in wild-type C57BL/6 (WT) mouse serum after (A) intraperitoneal (i.p.) infection with *EC* (10^7 cfu), (C) oral infection with *ST* (10^7 cfu), (E) i.p. infection with *SPN* (10^4 cfu), or (G) intravenous (i.v.) infection with *MRSA* (10^8 cfu).

(B, D, F, and H) Identical amounts of WT mouse serum protein (20 μg) were separated by SDS-PAGE and analyzed by protein staining with Coomassie brilliant blue (CBB) or by Western blotting with TNAP- and IAP-specific antibodies after infection with (B) *EC*, (D) *ST*, (F) *SPN*, or (H) *MRSA*. Quantification of the relative abundance of each AP isoform is plotted.

(I, J, Q, and T) Serum AP activity of WT mice receiving i.v. injections of cIAP (75 U/kg) at indicated times (arrows) following infection with (I) *EC*, (J) *ST*, (Q) *SPN*, or (T) *MRSA*.

(K and L) LPS abundance and phosphate amount released from LPS in serum of WT mice (K) 24 hr after *EC* infection or (L) 8 days after *ST* infection in the presence or absence of cIAP.

(M, N, R, and U) Serum inflammatory cytokine expression of WT mice receiving i.v. injections of cIAP following infection with (M) *EC*, (N) *ST*, (R) *SPN*, or (U) *MRSA*.

(O, P, S, and V) Survival of WT mice receiving i.v. injections of cIAP at indicated times (arrows) following infection with (O) *EC*, (P) *ST*, (S) *SPN*, or (V) *MRSA*.

In (A–N), (Q), (R), (T), and (U), n = 6 per condition. In (O) and (S), n = 12-15 per condition. In (P), n = 25 per condition. In (V), n = 10 per condition. Data are presented as means ± SEM from two independent experiments.

(AMR) (Ashwell and Morell, 1974), may be involved in the accelerated clearance of de-sialylated TNAP and IAP enzymes in the context of sepsis. In normal, uninfected animals, the multimeric AMR binds to de-sialylated multivalent glycan ligands bearing terminal galactose linkages, including those on TNAP and IAP, thereby regulating their half-lives and abundance by an intrinsic homeostatic and clearance mechanism (Yang et al., 2015). We observed that mice with a genetic deficiency of either the Asgr1 or Asgr2 chain of the AMR maintained elevated circulating AP activity and half-lives during sepsis caused by *EC* or *ST* (Figures 2G–2J), which was linked to the elevated abundance of circulating TNAP and IAP isozymes (Figures 2K and 2L). In the normal liver parenchyma, TNAP and IAP are mostly co-localized with Asgr1 and Asgr2 chains of the AMR, while their abundance in the liver is increased in sepsis caused by *ST* infection as well as diminished in the absence of either AMR chain (Figure S3). This is consistent with the increased half-lives and abundance of de-sialylated TNAP and IAP isozymes circulating in AMR deficiency.

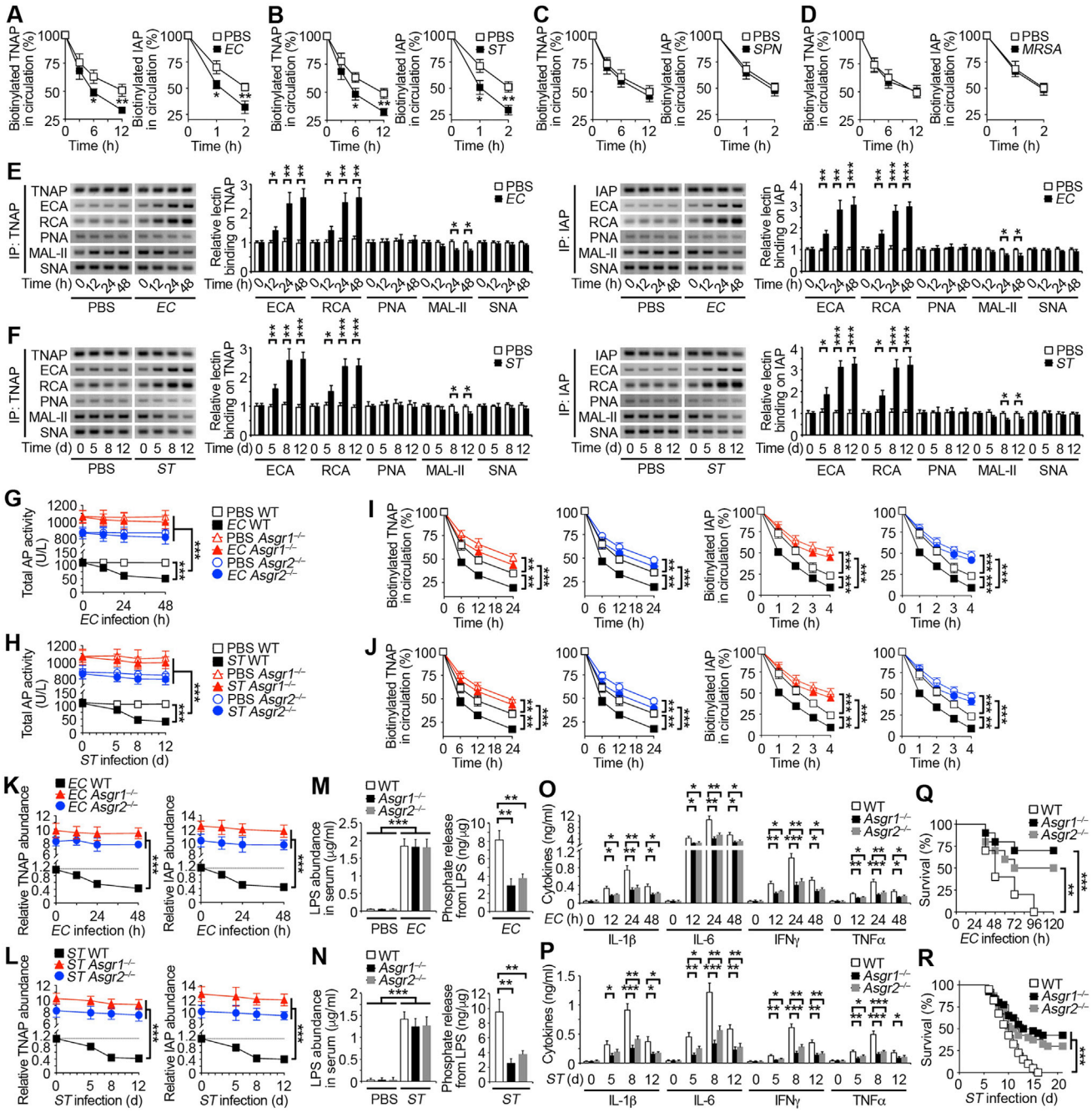

Figure 2. Accelerated Aging and Turnover of AP and the Role of the AMR in Maintaining AP Levels

(A–D) Half-life analyses of TNAP and IAP proteins in circulation of WT mouse serum (A) 24 hr after i.p. infection with *EC* (10^7 cfu), (B) day 8 after oral infection with *ST* (10^7 cfu), (C) 24 hr after i.p. infection with *SPN* (10^4 cfu), or (D) 24 hr after i.v. infection with *MRSA* (10^8 cfu) following biotinylation.

(E and F) Lectin blotting analyses are presented from identical amounts of TNAP and IAP isolated from WT mouse serum after (E) i.p. infection with *EC* (10^7 cfu) or (F) oral infection with *ST* (10^7 cfu).

(G and H) Total AP activity measured in AMR-deficient mouse serum after (G) i.p. infection with *EC* or (H) oral infection with *ST*. AMR is encoded by the *Asgr1* and *Asgr2* genes.

(I and J) Half-life analyses of TNAP and IAP proteins in circulation of AMR-deficient mouse serum (I) 24 h after infection with *EC* or (J) day 8 after infection with *ST* following biotinylation.

(K and L) TNAP and IAP abundance in AMR-deficient mouse serum after (K) i.p. infection with *EC* or (L) oral infection with *ST*.

(M and N) LPS abundance and phosphate amount released from LPS in serum of AMR-deficient mice (M) 24 hr after *EC* infection or (N) day 8 after *ST* infection.

(legend continued on next page)

Elevated AP Isozymes in AMR Deficiency Protect the Host during Sepsis Caused by Gram-Negative *EC* and *ST* Pathogens

Elevated bloodstream AP activity in AMR deficiency increased the ratio of de-phosphorylated to phosphorylated LPS during *EC* or *ST* sepsis concurrent with reduced inflammatory cytokine levels in circulation (Figures 2M–2P). In stark contrast to a protective role for host AMR function in *SPN* sepsis (Grewal et al., 2008, 2013), AMR deficiency was protective in sepsis caused by *EC* or *ST* (Figures 2Q and 2R). Selective inhibition of TNAP activity using the pharmacological inhibitor SBI-425 (Dahl et al., 2009; Pinkerton et al., 2018; Sheen et al., 2015) reduced total serum AP activity levels by over 70% on average among wild-type mice and their *Asgr*-null littermates, consistent with higher TNAP levels in circulation compared with IAP (Figures 3A and 3B). In sepsis caused by *EC* or *ST* pathogens, SBI-425 treatment of AMR-deficient mice similarly increased disease signs in measurements of LPS-phosphate levels, inflammation markers, and frequencies of survival (Figures 3C–3H), indicating a strong contribution of the TNAP isozyme to host protection. Among WT mice, there was a trend of increased disease signs measured with TNAP inhibition that did not acquire statistical significance. This likely reflects an overlapping role of IAP in normal host protection, which although expressed at much lower levels has a higher specific activity towards LPS (Kiffer-Moreira et al., 2014). We investigated further using Akp3-null mice (Narisawa et al., 2003) and observed that the greatest loss of AP activity in IAP deficiency occurred in the presence of SBI-425, which, as combined, promoted disease and mortality to the extent that *Asgr*-null mice were unable to survive sepsis caused by the *ST* pathogen (Figures 3I–3L). AP activity levels among normal, uninfected mice and their persistent elevation obtained by AMR deficiency conferred host protection in our sepsis protocols, while further AP augmentation among *Asgr*-null mice resulted in improvement (Figures 3M and 3N). In sepsis caused by *SPN* or *MRSA*, AMR deficiency had no protective effect, and instead appeared to shorten survival times similar to those reported previously using *SPN* (Grewal et al., 2008); this suggests that further studies may find AMR function to be protective to the host in *Staphylococcal* sepsis (Figures 3O and 3P). These findings together show that elevated AP levels in AMR deficiency are protective in sepsis caused by Gram-negative *EC* and *ST*, but not in sepsis caused by Gram-positive *SPN* or *MRSA*, and that both TNAP and IAP enzymes have host-protective roles in the former context.

ST3Gal6 Maintains AP Abundance in Providing Host Protection

Sialylation of TNAP and IAP occurs during their transit through the secretory pathway. Secreted proteins in the blood lose sialic acid linkages at distinct and measurable rates as they age in the presence of neuraminidase activity, resulting in their endocytic clearance by lectins such as the AMR (Yang et al., 2015). Among various sialyltransferase-deficient mice studied, those lacking the ST3Gal6 sialyltransferase had diminished blood AP activity with corresponding deficits of TNAP and IAP abundance (Figures 4A and 4B), while TNAP or IAP mRNA levels were unaltered (Figure S4A). Reduced AP activity in ST3Gal6 deficiency was further linked to a reduction of sialic acid linkages on TNAP and IAP, coincident with increased exposure of underlying galactose linkages and diminished half-lives of both AP isozymes (Figures 4C and 4D).

Sepsis caused by *EC* or *ST* infection further diminished AP activity and TNAP and IAP abundance in ST3Gal6 deficiency, wherein glycan remodeling evidenced by diminished sialic acid linkages and unmasked galactose linkages was further amplified (Figures 4E–4J). Moreover, ST3Gal6 deficiency contributed to marked reductions of TNAP and IAP half-lives during sepsis (Figures 4K and 4L). Augmentation with cIAP boosted blood AP activity levels among *St3gal6*-null mice and lowered the phosphorylation level of LPS present during sepsis with reduced inflammatory cytokine levels and improved host survival (Figures 4M–4T). In contrast, frequencies of death were unaltered among *St3gal6*-null mice in sepsis caused by Gram-positive *SPN* or *SA* (Figures S4B and S4C). The opposing effects of ST3Gal6 (glycoprotein sialylation) and the AMR (endocytic clearance of de-sialylated glycoproteins) were further investigated in mice genetically deficient in both components. The AMR effect was dominant, as expected, with continued elevation of AP activity and increased abundance of TNAP and IAP bearing diminished sialic acid linkages in ST3Gal6 co-deficiency, coincident with increased frequencies of host survival (Figures S4D–S4I). These findings indicated an interaction between ST3Gal6 and the AMR in controlling AP homeostasis and host protection in sepsis caused by Gram-negative *EC* and *ST* pathogens. How *EC* and *ST* trigger a reduction of sialic acid linkages on circulating TNAP and IAP in compromising this mechanism of host protection was next investigated.

Toll-like Receptor 4 (TLR4)-Dependent Induction of Host Neuraminidases in Sepsis Caused by Gram-Negative *EC* and *ST* Pathogens

Neuraminidase (Neu) activity cleaves sialic acid linkages, thereby exposing underlying galactose ligands of the AMR among host glycoproteins. Some neuraminidases are encoded by pathogens as virulence factors; however, no neuraminidases reside in the genomes of the *EC* and *ST* isolates used herein (Figueroa-Bossi et al., 2001; Russo et al., 1990; Vimr and Troy, 1985). The de-sialylation of TNAP and IAP during sepsis therefore implied the presence and induction of host Neu activity, with consequent decreased AP isozyme abundance leading to increases of LPS-phosphate and resulting Toll-like receptor 4 (TLR4) activation of innate immune responses causing inflammation (Beutler, 2000; Poltorak et al., 1998).

(O and P) Serum inflammatory cytokine expression in AMR-deficient mouse serum following (O) i.p. infection with *EC* or (P) oral infection with *ST*.
(Q and R) Survival of AMR-deficient mice following (Q) i.p. infection with *EC* or (R) oral infection with *ST*.
In (A–D), (I), and (J), n = 8 per condition. In (E–H) and (K–P), n = 6 per condition. In (Q), n = 20 per condition. In (R), n = 40 per condition. Data are presented as means ± SEM from two independent experiments.

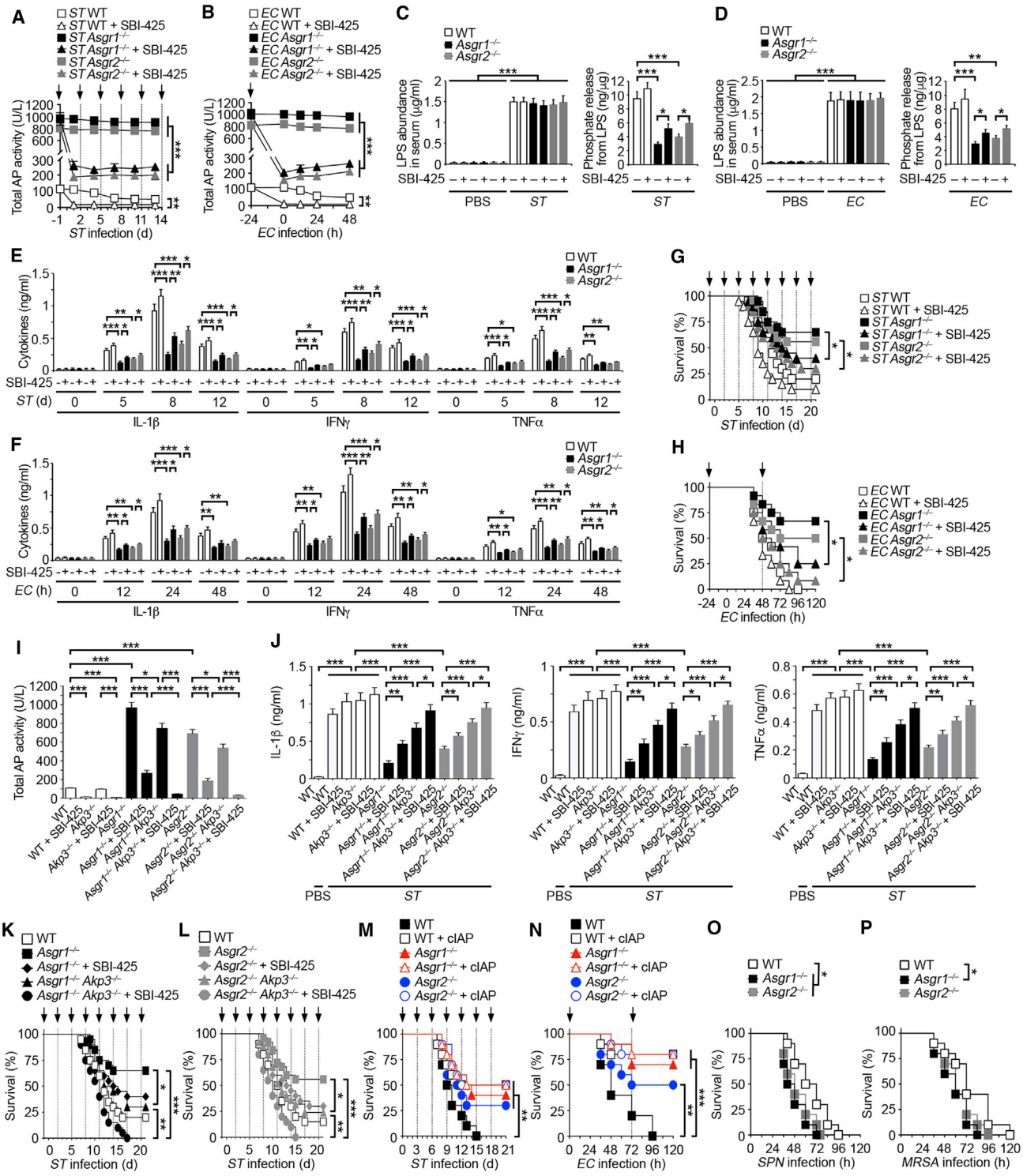

Figure 3. Effects of AP Inhibition in AMR Deficiency and Sepsis

(A and B) Total AP activity measured in the serum of indicated genotypes after (A) oral infection with *ST* (10^7 cfu) or (B) i.p. infection with *EC* (10^7 cfu) in the absence and presence of TNAP inhibitor SBI-425 (10 mg/kg) at indicated times (arrows).

(C and D) LPS abundance and phosphate amount released from LPS in serum of indicated genotypes (C) 8 days after *ST* infection or (D) 24 hr after *EC* infection in the presence or absence of SBI-425.

(E and F) Serum inflammatory cytokine expression of indicated genotypes after (E) oral infection with *ST* (10^7 cfu) or (F) i.p. infection with *EC* (10^7 cfu) in the absence and presence of SBI-425.

(legend continued on next page)

We detected the presence of a TLR4-dependent mechanism that elevated blood Neu activity during sepsis caused by *ST* and *EC* (Figures 5A and 5B). Among the four Neu isozymes encoded by mammalian genomes (Neu1–Neu4), only Neu1 and Neu3 have been detected in blood circulation (Yang et al., 2015). Both Neu1 and Neu3 are widely expressed among cell types and may be secreted into circulation by lysosomal, exosomal, or proteolytic mechanisms. In sepsis caused by *EC* or *ST* infections, the expression of both Neu1 and Neu3 in circulation was induced in a TLR4-dependent manner (Figures 5C and 5D). In contrast, elevated blood Neu activity detected in *SPN* sepsis was independent of TLR4 function and occurred without changes in the abundance of Neu1 and Neu3, consistent with expression of the pathogen-encoded neuraminidase NanA (Grewal et al., 2008; Figures 5E and 5F). No changes were found in overall Neu activity or the abundance of circulating Neu1 and Neu3 in similar studies with *MRSA* (Figures 5G and 5H). TLR4-dependent reductions of AP activity and abundance in sepsis caused by Gram-negative *EC* and *ST* pathogens were linked to diminished TNAP and IAP half-lives in circulation, concurrent with reductions of sialic acid linkages and exposure of underlying galactose ligands (Figures 5I, 5J, and S5A–S5D). TLR4 deficiency was further associated with reductions of phosphate levels on circulating LPS and inflammatory cytokine expression (Figures 5K–5N). Moreover, the frequency of survival was significantly increased in the absence of TLR4 function (Figures 5O and 5P), while cIAP treatment of the TLR4-deficient mice had no significant additional protective effect (Figures S5E and S5F). These findings reveal a TLR4-dependent mechanism that elevates host Neu1 and Neu3 levels in circulation during sepsis caused by Gram-negative *EC* or *ST* infections, consequently diminishing AP activity, reducing TNAP and IAP abundance, promoting inflammation, and increasing mortality.

LPS Recapitulates Host TLR4-Dependent Neu Induction in Provoking Pathogenesis

The suspected role of LPS produced by Gram-negative *EC* and *ST* pathogens in TLR4-dependent induction of host Neu1 and Neu3 was probed. Intraperitoneal administration of *E. coli* LPS obtained from commercial sources resulted in elevated Neu activity in circulation in a TLR4-dependent manner coincident with increased abundance of Neu1 and Neu3 (Figures 5Q and 5R). LPS administration reduced circulating AP activity and diminished TNAP and IAP levels (Figure 5S) without altering TNAP or IAP transcript abundance, instead diminishing half-lives of AP isozymes in circulation with exposure of underlying endocytic galactose linkages (Figures 5T and S6A–S6C). Phosphorylated LPS and inflammatory cytokine expression were concurrently increased in the presence of TLR4 function, while TLR4 deficiency resulted in reduced LPS-phosphate levels, diminished inflammatory cytokine induction, and increased frequencies of host survival (Figures 5U–5W). Augmentation of AP activity by cIAP treatment was further therapeutic in the LPS challenge model (Figures S6D–S6G). Similarly, elevated AP levels in AMR deficiency lessened susceptibility to LPS with reduced LPS-phosphate, diminished inflammatory cytokine expression, and improved host survival (Figures S6H–S6L). Correspondingly, ST3Gal6 deficiency increased susceptibility to LPS toxicity, with further reductions of AP activity and isozyme half-lives resulting in increased LPS-phosphate, elevated inflammatory cytokine expression, and reduced host survival, all of which were modulated as expected by cIAP treatment or by AMR co-deficiency (Figures S6M–S6S).

Neu Inhibition Sustains AP Function and Limits LPS-Mediated Pathology in Sepsis

The induction of host Neu activity by LPS and TLR4 was linked to increased inflammatory cytokine expression and mortality, implying that Neu inhibitors may be of therapeutic value in sepsis caused by the Gram-negative *EC* and *ST* pathogens. We investigated whether Neu inhibitors representing anti-viral compounds and marketed drugs including 2,3-dehydro-2-deoxy-N-acetylneuraminic acid (DANA) and Zanamivir (tradename Relenza) could maintain AP levels and thereby provide host protection.

DANA or Zanamivir was administered immediately following *EC* or *ST* infections and every 24 hr thereafter. Marked inhibition of blood Neu activity was achieved with either inhibitor; this resulted in circulating Neu activity levels comparable to uninfected animals, which coincided with retentions of basal AP activity, TNAP and IAP abundance, and sialic acid linkages (Figures 6A–6H). Treatment with DANA or Zanamivir also lowered circulating levels of LPS-phosphate during sepsis, blunting inflammatory cytokine expression and markedly improving host survival (Figures 6I–6N). Notably, inhibition of circulating Neu activity during *SPN* or *MRSA* sepsis did not diminish disease marked by elevated inflammatory cytokines and reduced survival (Figures 6O–6R). Similar studies of Neu inhibition in LPS administration further revealed therapeutic effects linked to the retention of sialic acid linkages, circulating AP levels, LPS de-phosphorylation, reduced inflammatory cytokines, and increased host survival (Figure S7). These findings together indicate the presence of a mechanism of host protection against sepsis caused by Gram-negative *EC* and *ST* pathogens that is dysregulated by signals linked to TLR4 function and that can be reinforced by AP augmentation or Neu inhibition.

(G and H) Survival of indicated genotypes following (G) oral infection with *ST* (10^6 cfu) or (H) i.p. infection with *EC* (10^7 cfu) in the absence and presence of SBI-425 (arrows).
(I) Total AP activity measured in the serum of indicated genotypes 24 hr after i.p. injection with SBI-425.
(J) Serum inflammatory cytokine expression of indicated genotypes 8 days after oral infection with *ST* (10^7 cfu) in the absence and presence of SBI-425.
(K and L) Survival of indicated genotypes following oral infection with *ST* (10^6 cfu) in the absence and presence of SBI-425 at indicated times (arrows).
(M and N) Survival of AMR-deficient mice receiving i.v. injections of cIAP (75 U/kg) at indicated times (arrows) following (M) oral infection with *ST* (10^7 cfu) or (N) i.p. infection with *EC* (10^7 cfu).
(O and P) Survival of AMR-deficient mice following (O) i.p. infection with *SPN* (10^4 cfu) or (P) i.v. infection with *MRSA* (10^8 cfu).
In (A–F), n = 6 per condition. In (G), (H), (K), and (L), n = 20-25 per condition. In (I), n = 10 per condition. In (J), n = 8 per condition. In (M–P), n = 10-12 per condition. Data are presented as means ± SEM from two independent experiments.

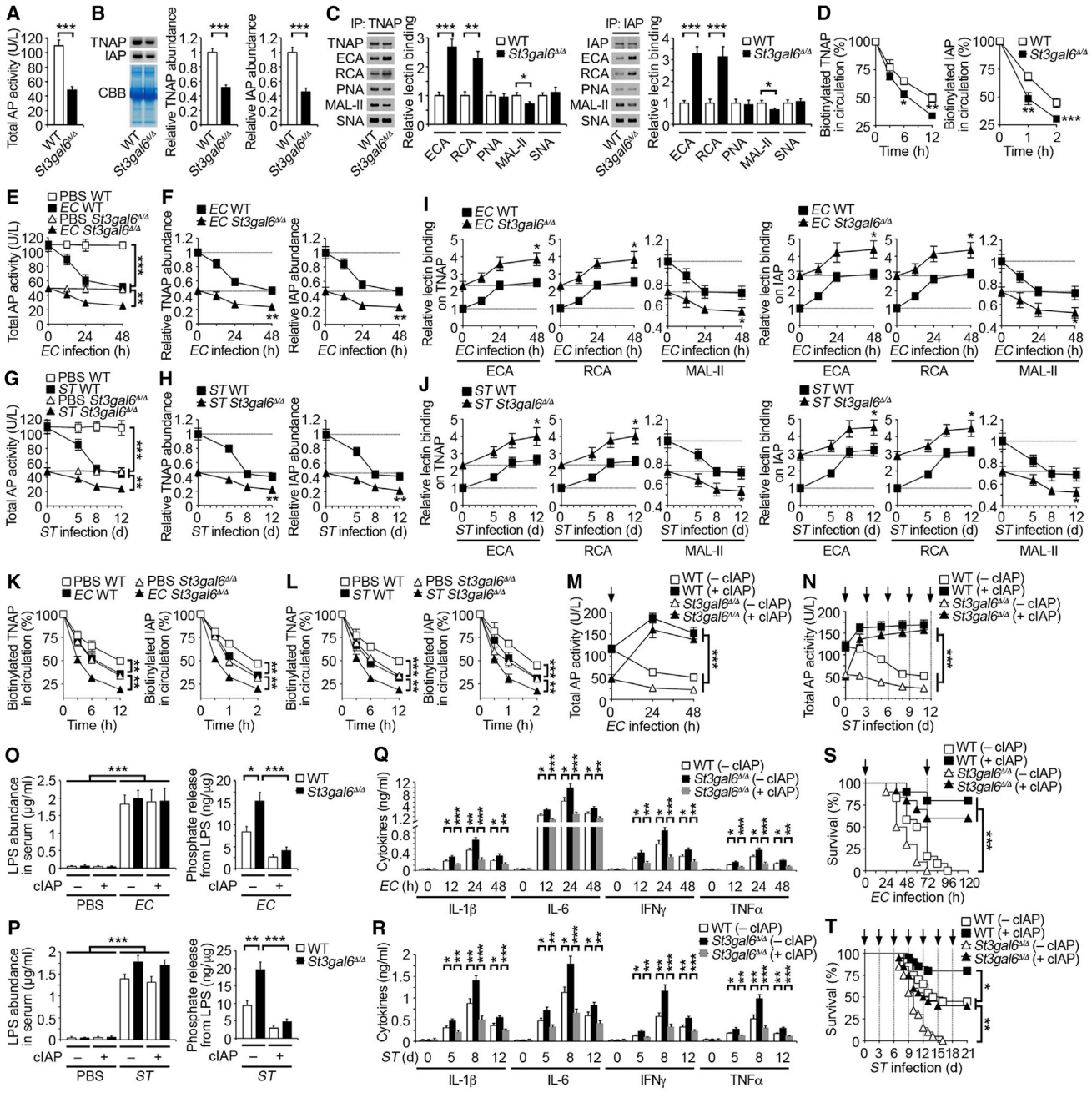

Figure 4. Role of AP Sialylation by ST3Gal6 Sialyltransferase in Isozyme Homeostasis

(A and B) Total AP activity (A) and TNAP and IAP abundance (B) measured in ST3Gal6-deficient mouse serum. ST3Gal6 is encoded by the *St3gal6* gene.

(C) Lectin blotting analyses are presented from identical amounts of TNAP and IAP isolated from sera of ST3Gal6-deficient mice.

(D) Half-life analyses of TNAP and IAP glycoproteins in circulation of ST3Gal6-deficient mouse serum following biotinylation.

(E and G) Total AP activity measured in ST3Gal6-deficient mouse serum after (E) i.p. infection with *EC* (10^7 cfu) or (G) oral infection with *ST* (10^7 cfu).

(F and H) TNAP and IAP abundance measured in ST3Gal6-deficient mouse serum after (F) i.p. infection with *EC* (10^7 cfu) or (H) oral infection with *ST* (10^7 cfu).

(I and J) Lectin binding on TNAP and IAP proteins isolated from ST3Gal6-deficient mouse serum after infection with (I) *EC* (10^7 cfu) or (J) *ST* (10^7 cfu).

(K and L) Half-life analyses of TNAP and IAP glycoproteins in circulation of ST3Gal6-deficient mouse serum (K) 24 hr after infection with *EC* (10^7 cfu) or (L) on day 8 after infection with *ST* (10^7 cfu) following biotinylation.

(M and N) Serum AP activity of ST3Gal6-deficient mice receiving i.v. injections of cIAP (75 U/kg) at indicated times (arrows) following infection with (M) *EC* (10^7 cfu) or (N) *ST* (10^7 cfu).

(O and P) LPS abundance and phosphate amount released from LPS in serum of ST3Gal6-deficient mice (O) 24 hr after *EC* infection (10^7 cfu) or (P) on day 8 after *ST* infection (10^7 cfu) in the presence or absence of cIAP.

(Q and R) Serum inflammatory cytokine expression in ST3Gal6-deficient mouse serum following infection with (Q) *EC* (10^7 cfu) or (R) *ST* (10^7 cfu).

(legend continued on next page)

DISCUSSION

Originating from infections caused by disparate agents including bacteria, fungi, and viruses, host responses in sepsis commonly elicit excessive inflammation and coagulopathy, determining pathological severity and mortality (Stearns-Kurosawa et al., 2011). Commonalities identified in the pathways driving tissue injury and organ dysfunction have not precluded the potential for distinct pathogenic mechanisms operating at the onset of host responses to specific microbes, the identification of which may provide stratification to guide individualized therapeutic interventions prior to the manifestation of severe disease. From our comparative studies of distinct Gram-positive bacterial pathogens such as *SPN* and *SA* and Gram-negative bacterial pathogens such as *EC* and *ST*, we have identified a selective mechanism of host protection against LPS toxicity that is targeted by Gram-negative *EC* and *ST* pathogens. *EC* is a common cause of human sepsis worldwide, with increasing problems of antibiotic resistance (Poolman and Wacker, 2016) while nontyphoidal *ST* is a leading cause of bacteremia in sub-Saharan Africa, with an associated case mortality of 25% (de Jong et al., 2012; Feasey et al., 2012). In more developed countries, recurrent *ST* infections are a leading cause of food poisoning and may increase the potential for the development of colitis (Yang et al., 2017). In the present study, we found that *ST* and *EC* pathogens selectively target and disrupt a mechanism of host protection by activating TLR4 to increase circulating levels of Neu1 and Neu3, implicating similar pathogenic mechanisms as operating in sepsis and colitis. Elevated Neu activity accelerated the molecular aging and endocytic clearance of circulating anti-inflammatory isozymes TNAP and IAP by the hepatic AMR, diminishing the host capacity for LPS de-phosphorylation and de-toxification and thereby promoting TLR4-dependent inflammation with reduced likelihood of host survival.

Using pharmacological and genetic approaches to discriminate among AP isozyme function, we determined that both TNAP and IAP contributed substantially to host protection against LPS toxicity in sepsis. Failure of the host to establish or maintain post-translational control of AP isozyme abundance in the blood had severe consequences and could also manifest by ST3Gal6 sialyltransferase deficiency with failure to adequately sialylate AP isozymes during isozyme synthesis; in contrast, AMR deficiency was strongly protective by maintenance of high levels of AP isozymes that would normally have been cleared following de-sialylation with increased molecular age. Notably, this contrasts with AMR function in providing host protection during *SPN* sepsis (Grewal et al., 2008 and 2013), together placing the AMR at a nexus of host response pathways differentially influencing the outcomes of sepsis.

Differences detected in responses of the host to sepsis caused by Gram-positive *SPN* and *SA* pathogens compared with Gram-negative *EC* and *ST* pathogens centered in this study on the regulation of circulating host neuraminidases. The functions of mammalian neuraminidases and other glycosidases are under increased scrutiny and have been recently shown to contribute to an intrinsic mechanism of protein aging involving rates of glycan remodeling including de-sialylation that generate endocytic lectin ligands in determining secreted and cell surface protein half-lives, abundance, and thereby function (Yang et al., 2015 and 2017). In previous studies of the host response to Gram-positive *SPN* sepsis, where de-toxification of LPS was not a consideration, the de-sialylation of platelets by the *SPN* NanA neuraminidase benefitted the host in the context of sepsis. NanA-mediated platelet de-sialylation was detected by the host, resulting in AMR-dependent platelet clearance and producing an essential moderate thrombocytopenia that moderated an otherwise invariably lethal form of disseminated intravascular coagulation (Grewal et al., 2008 and 2013). Neither of the Gram-positive *SA* strains studied herein, which both lack neuraminidase genes, caused an appreciable change in circulating Neu activity in the host. Moreover, AP augmentation had no untoward effects to the host during sepsis caused by the Gram-positive *SPN* and *SA* pathogens studied. In contrast, the increase in circulating Neu1 and Neu3 caused by Gram-negative *ST* and *EC* pathogens in the presence of host TLR4 accelerated the rate of TNAP and IAP de-sialylation, increasing AMR-dependent clearance, impairing LPS de-toxification, and thereby elevating TLR4-dependent inflammation. The de-phosphorylation of LPS by AP activity was only therapeutic in the context of TLR4 function, and thus AP treatment was beneficial to WT but not TLR4-deficient hosts. Our results, including maximal survival frequencies in these protocols, also support the view that additional unidentified mechanisms remain that are unrelated to AP modulation and are involved in the pathogenesis of Gram-negative sepsis.

Discoveries of dissimilar biomarkers elicited early in host responses to different pathogens may begin to stratify sepsis patients for earlier, targeted treatment approaches that block the emergence of common downstream pathologies spanning hyperinflammation, thrombosis, and hypoperfusion. The clinical utility of unique pathogenic biomarkers will likely depend upon advances in patient fluid culture-independent diagnostic modalities to confirm pathogen locations and identities early in the onset of sepsis. We have identified a post-translational mechanism of AP isozyme regulation that is targeted by Gram-negative *EC* and *ST* bacterial pathogens early in the progression of sepsis. The resulting disruption of host protection by acquired AP deficiency increased host sensitivity to the bacterial LPS toxin through TLR4-mediated inflammation. Therapeutic intervention to maintain normal AP abundance by AP augmentation or by Neu inhibition were each highly effective in suppressing TLR4-dependent inflammation and reducing mortality. Clinical trials with AP augmentation in humans have similarly indicated anti-inflammatory effects in the settings of post-cardiopulmonary surgery, ulcerative colitis, and sepsis, while genetic deficiency of IAP in humans has been linked with colitis (Heemskerk et al., 2009; Kats et al., 2009; Lukas et al., 2010; Parlato et al., 2018; Peters et al., 2015; Pickkers et al., 2012). Clinical approaches

(S and T) Survival of ST3Gal6-deficient mice receiving i.v. injections of cIAP at indicated times (arrows) following infection with (S) *EC* (10^7 cfu) or (T) *ST* (5×10^5 cfu).

In (A), (C), (E–J), and (M–R), n = 6 per condition. In (B), (D), (K), and (L), n = 8 per condition. In (S), n = 12 per condition. In (T), n = 20 per condition. Data are presented as means ± SEM from two independent experiments.

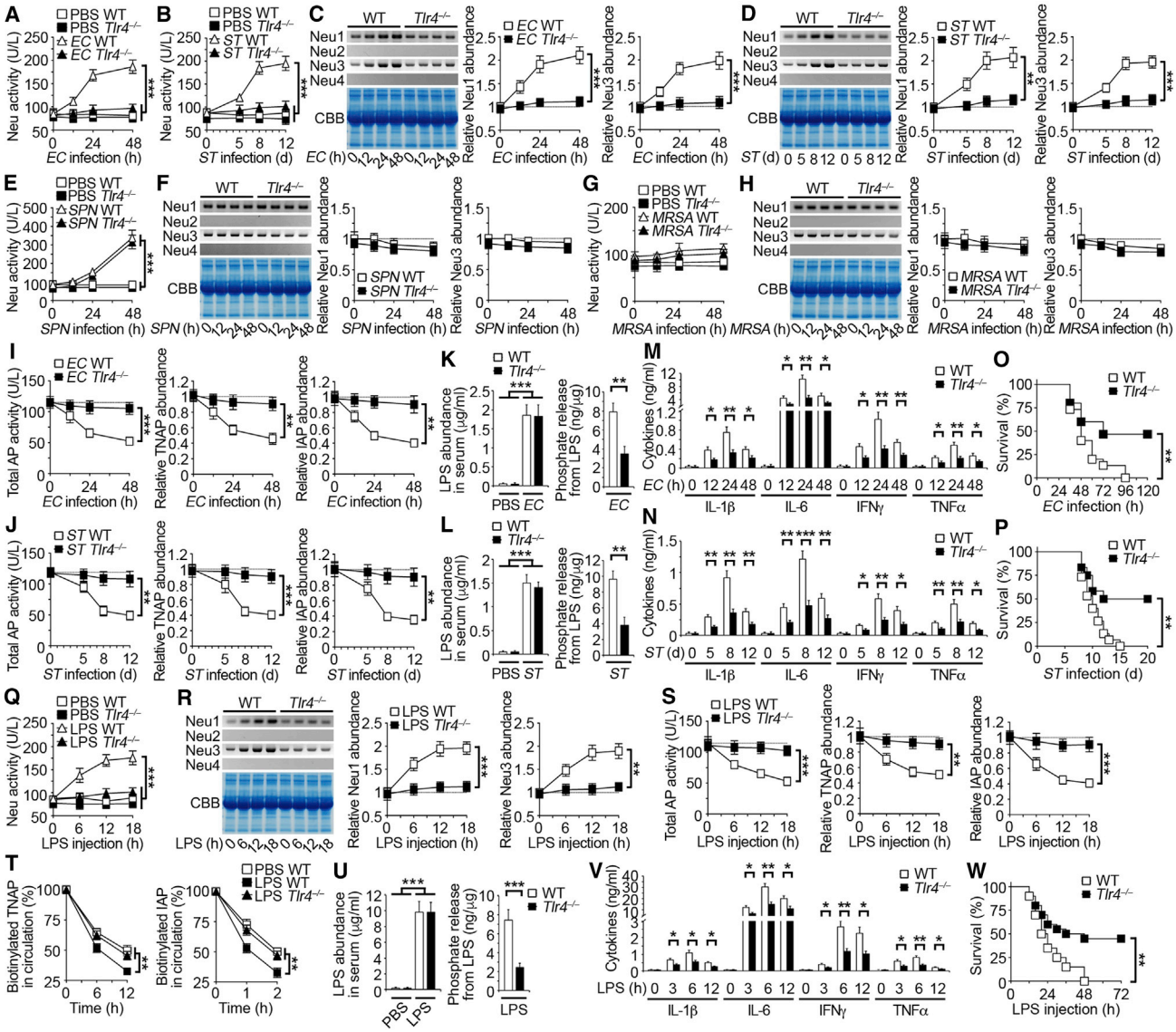

Figure 5. Inductions of Host Neuraminidases by TLR4 and LPS Control AP Sialylation and Abundance in the Pathophysiology of Sepsis

(A, B, E, and G) Total neuraminidase (Neu) activity measured in TLR4-deficient mouse serum after (A) i.p. infection with *EC* (10^7 cfu), (B) oral infection with *ST* (10^7 cfu), (E) i.p. infection with *SPN* (10^4 cfu), or (G) i.v. infection with *MRSA* (10^8 cfu).

(C, D, F, and H) Antibodies specific to Neu1, Neu2, Neu3, or Neu4 were used to detect Neu protein abundance in TLR4-deficient mouse serum after infection with (C) *EC*, (D) *ST*, (F) *SPN*, or (H) *MRSA* by western blotting. Quantification of the relative abundance of each protein sample is plotted.

(I and J) Total AP activity and TNAP and IAP abundance measured in TLR4-deficient mouse serum after infection with (I) *EC* or (J) *ST*.

(K and L) LPS abundance and phosphate amount released from LPS in serum of TLR4-deficient mice on (K) 24 hr after *EC* infection or (L) on day 8 after *ST* infection.

(M and N) Serum inflammatory cytokine expression in TLR4-deficient mouse serum following infection with (M) *EC* or (N) *ST*.

(O and P) Survival of TLR4-deficient mice following infection with (O) *EC* or (P) *ST*.

(Q and R) Total Neu activity (Q) and Neu1, 2, 3 and 4 abundance (R) measured in TLR4-deficient mouse serum after i.p. injection with LPS (40 mg/kg; *EC* 0111:B4).

(S) Total AP activity and TNAP and IAP abundance in TLR4-deficient mouse serum after i.p. injection with LPS.

(T) Half-life analyses of TNAP and IAP glycoproteins in circulation of TLR4-deficient mouse serum 12 hr after i.p. injection with LPS following biotinylation.

(U) LPS abundance and phosphate amount released from LPS in serum of TLR4-deficient mice 12 hr after LPS injection.

(V) Serum inflammatory cytokine expression of TLR4-deficient mice following i.p. injection with LPS.

(W) Survival of TLR4-deficient mice following i.p. injection with LPS.

In (A–N), (Q–S), (U), and (V), n = 6 per condition. In (O and P), n = 12–15 per condition. In (T), n = 8 per condition. In (W), n = 20 per condition. Data are presented as means ± SEM from two independent experiments.

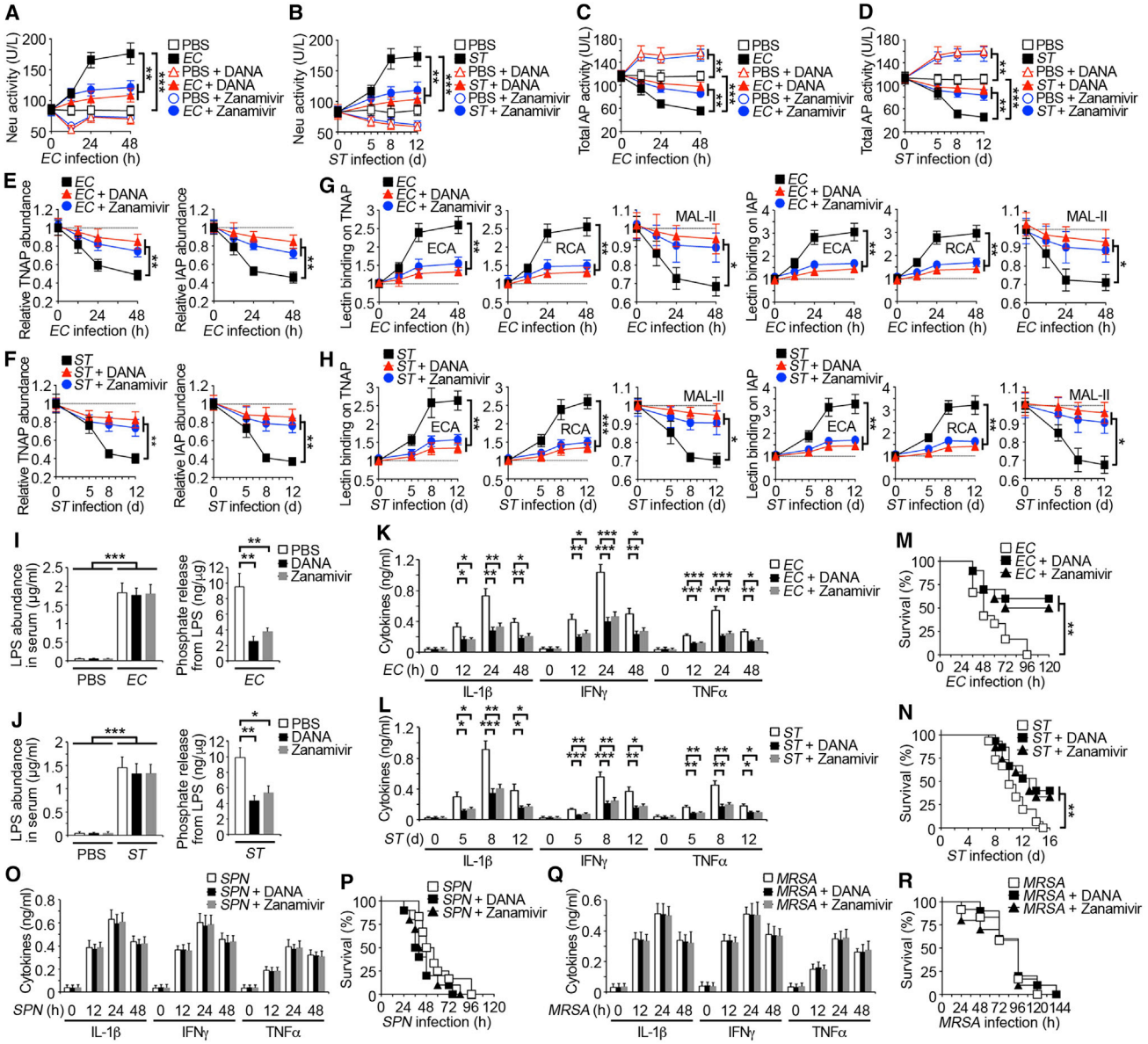

Figure 6. Effects of Neuraminidase Inhibitors in Sepsis

(A and B) Total Neu activity measured in WT mouse serum after (A) i.p. infection with *EC* (10^7 cfu) or (B) oral infection with *ST* (10^7 cfu) in the absence or presence of the broad-spectrum neuraminidase inhibitor DANA (2,3-dehydro-2-deoxy-*N*-acetylneuraminic acid, 250 mg/kg, every 24 hr) or Zanamivir (250 mg/kg, every 24 hr).

(C and D) Total AP activity measured in WT mouse serum after infection with (C) *EC* or (D) *ST* in the absence or presence of DANA or Zanamivir.

(E and F) TNAP and IAP abundance measured in WT mouse serum after infection with (E) *EC* or (F) *ST* in the absence or presence of DANA or Zanamivir.

(G and H) Lectin binding analyses of TNAP and IAP isolated from WT mouse serum after infection with (G) *EC* or (H) *ST* in the absence or presence of DANA or Zanamivir.

(I and J) LPS abundance and phosphate amount released from LPS in serum of WT mice (I) 24 hr after *EC* infection or (J) on day 8 after *ST* infection in the presence or absence of DANA or Zanamivir.

(K, L, O, Q) Serum inflammatory cytokine expression in WT mouse serum following infection with (K) *EC*, (L) *ST*, (O) *SPN*, or (Q) *MRSA* in the absence or presence of DANA or Zanamivir.

(M, N, P, and R) Survival of WT mice following infection with (M) *EC*, (N) *ST*, (P) *SPN*, or (R) *MRSA* in the absence or presence of DANA or Zanamivir.

In (A–L), (O), and (Q), n = 6 per condition. In (M), (P), and (R), n = 12 per condition. In (N), n = 15 per condition. Data are presented as means ± SEM from two independent experiments.

to block TLR4 signaling for therapeutic benefit have been unsuccessful thus far, however. Neither the LPS analog Eritoran nor the small molecule TAK-242 were able to reduce inflammatory cytokine responses and alter outcomes in patients diagnosed with sepsis (Opal et al., 2013; Rice et al., 2010). This may reflect difficulties in the therapeutic delivery of each compound or the

possibility that human TLR4 complexes are structurally dissimilar from those in the mouse, wherein each compound was tested. Impeding TLR4 signaling in sepsis by AP-mediated dephosphorylation of LPS represents a cogent therapeutic approach, wherein Gram-negative pathogens may otherwise dismantle this mechanism of host protection by depleting anti-inflammatory AP isozymes.

STAR★METHODS

Detailed methods are provided in the online version of this paper and include the following:

- KEY RESOURCES TABLE
- CONTACT FOR REAGENT AND RESOURCE SHARING
- EXPERIMENTAL MODEL AND SUBJECT DETAILS
  - Laboratory Animals
  - Bacterial Strains and Culture Conditions
- METHOD DETAILS
  - Bacterial Infections
  - Blood Chemistry and Calf Intestinal Alkaline Phosphatase Treatment
  - Glycoprotein Immunoprecipitation, Western Blotting, and Lectin Blotting
  - Enzyme-Linked Immunosorbent Assay and Serum Cytokine Measurements
  - LPS Phosphorylation
  - Blood Glycoprotein Half-Life
  - Neuraminidase Activity and Inhibition
  - TNAP Inhibition
  - LPS-induced Toxicity
  - mRNA Analyses
  - Histology
  - Experimental Design
- QUANTIFICATION AND STATISTICAL ANALYSIS

SUPPLEMENTAL INFORMATION

Supplemental Information includes seven figures and can be found with this article online at https://doi.org/10.1016/j.chom.2018.09.011.

ACKNOWLEDGMENTS

This research was funded by NIH grants HL125352 (J.D.M. and V.N.) and HL131474 (J.D.M., M.J.M., and V.N.). Additional support was provided by the Swedish Research Council 2017-00192 (J.S.W.).

AUTHOR CONTRIBUTIONS

W.H.Y., D.M.H., P.V.A., B.H.-G., J.S.W., M.J.M., and J.D.M. designed the experimental strategies. J.D.M. supervised the project. W.H.Y., D.M.H., P.V.A., B.H.-G., and J.S.W. performed the experiments and acquired data. W.H.Y., D.M.H., P.V.A., B.H.-G., J.S.W, S.N., A.B.P., J.L.M., V.N., M.J.M, and J.D.M. contributed to data analysis and manuscript preparation.

DECLARATION OF INTERESTS

The authors declare no conflicts of interest.

Received: June 18, 2018
Revised: August 9, 2018
Accepted: September 16, 2018
Published: October 10, 2018

REFERENCES

Ashwell, G., and Morell, A. (1974). The dual role of sialic acid in the hepatic recognition and catabolism of serum glycoproteins. Biochem. Soc. Symp. *40*, 117–124.

Bates, J.M., Akerlund, J., Mittge, E., and Guillemin, K. (2007). Intestinal alkaline phosphatase detoxifies lipopolysaccharide and prevents inflammation in zebrafish in response to the gut microbiota. Cell Host Microbe *2*, 371–382.

Bentala, H., Verweij, W.R., Huizinga-Van der Vlag, A., van Loenen-Weemaes, A.M., Meijer, D.K., and Poelstra, K. (2002). Removal of phosphate from lipid A as a strategy to detoxify lipopolysaccharide. Shock *18*, 561–566.

Beumer, C., Wulferink, M., Raaben, W., Fiechter, D., Brands, R., and Seinen, W. (2003). Calf intestinal alkaline phosphatase, a novel therapeutic drug for lipopolysaccharide (LPS)-mediated diseases, attenuates LPS toxicity in mice and piglets. J. Pharmacol. Exp. Ther. *307*, 737–744.

Beutler, B. (2000). Endotoxin, toll-like receptor 4, and the afferent limb of innate immunity. Curr. Opin. Microbiol. *3*, 23–28.

Chang, H.J., Lynm, C., and Glass, R.M. (2010). JAMA patient page. Sepsis. JAMA *304*, 1856.

Chaudhry, H., Zhou, J., Zhong, Y., Ali, M.M., McGuire, F., Nagarkatti, P.S., and Nagarkatti, M. (2013). Role of cytokines as a double-edged sword in sepsis. In Vivo *27*, 669–684.

Chow, O.A., von Köckritz-Blickwede, M., Bright, A.T., Hensler, M.E., Zinkernagel, A.S., Cogen, A.L., Gallo, R.L., Monestier, M., Wang, Y., Glass, C.K., and Nizet, V. (2010). Statins enhance formation of phagocyte extracellular traps. Cell Host Microbe *8*, 445–454.

Cross, A.S., Hyun, S.W., Miranda-Ribera, A., Feng, C., Liu, A., Nguyen, C., Zhang, L., Luzina, I.G., Atamas, S.P., Twaddell, W.S., et al. (2012). NEU1 and NEU3 sialidase activity expressed in human lung microvascular endothelia: NEU1 restrains endothelial cell migration, whereas NEU3 does not. J. Biol. Chem. *287*, 15966–15980.

D'Elia, R.V., Harrison, K., Oyston, P.C., Lukaszewski, R.A., and Clark, G.C. (2013). Targeting the "cytokine storm" for therapeutic benefit. Clin. Vaccine Immunol. *20*, 319–327.

Dahl, R., Sergienko, E.A., Su, Y., Mostofi, Y.S., Yang, L., Simao, A.M., Narisawa, S., Brown, B., Mangravita-Novo, A., Vicchiarelli, M., et al. (2009). Discovery and validation of a series of aryl sulfonamides as selective inhibitors of tissue-nonspecific alkaline phosphatase (TNAP). J. Med. Chem. *52*, 6919–6925.

Davis, M.R., Jr., and Goldberg, J.B. (2012). Purification and visualization of lipopolysaccharide from Gram-negative bacteria by hot aqueous-phenol extraction. J. Vis. Exp. *63*, 3916.

de Jong, H.K., Parry, C.M., van der Poll, T., and Wiersinga, W.J. (2012). Host-pathogen interaction in invasive Salmonellosis. PLoS Pathog. *8*, e1002933.

Dejager, L., Pinheiro, I., Dejonckheere, E., and Libert, C. (2011). Cecal ligation and puncture: the gold standard model for polymicrobial sepsis? Trends Microbiol. *19*, 198–208.

Ellies, L.G., Ditto, D., Levy, G.G., Wahrenbrock, M., Ginsburg, D., Varki, A., Le, D.T., and Marth, J.D. (2002). Sialyltransferase ST3Gal-IV operates as a dominant modifier of hemostasis by concealing asialoglycoprotein receptor ligands. Proc. Natl. Acad. Sci. USA *99*, 10042–10047.

Feasey, N.A., Dougan, G., Kingsley, R.A., Heyderman, R.S., and Gordon, M.A. (2012). Invasive non-typhoidal salmonella disease: an emerging and neglected tropical disease in Africa. Lancet *379*, 2489–2499.

Figueroa-Bossi, N., Uzzau, S., Maloriol, D., and Bossi, L. (2001). Variable assortment of prophages provides a transferable repertoire of pathogenic determinants in Salmonella. Mol. Microbiol. *39*, 260–271.

Fleischmann, C., Scherag, A., Adhikari, N.K., Hartog, C.S., Tsaganos, T., Schlattmann, P., Angus, D.C., and Reinhart, K.; International Forum of Acute Care Trialists (2016). Assessment of global incidence and mortality of hospital-treated sepsis. Current estimates and limitations. Am. J. Respir. Crit. Care Med. *193*, 259–272.

Gaieski, D.F., Edwards, J.M., Kallan, M.J., and Carr, B.G. (2013). Benchmarking the incidence and mortality of severe sepsis in the United States. Crit. Care Med. *41*, 1167–1174.

Goldberg, R.F., Austen, W.G., Jr., Zhang, X., Munene, G., Mostafa, G., Biswas, S., McCormack, M., Eberlin, K.R., Nguyen, J.T., Tatlidede, H.S., et al. (2008). Intestinal alkaline phosphatase is a gut mucosal defense factor maintained by enteral nutrition. Proc. Natl. Acad. Sci. USA *105*, 3551–3556.

Grewal, P.K., Uchiyama, S., Ditto, D., Varki, N., Le, D.T., Nizet, V., and Marth, J.D. (2008). The Ashwell receptor mitigates the lethal coagulopathy of sepsis. Nat. Med. *14*, 648–655.

Grewal, P.K., Aziz, P.V., Uchiyama, S., Rubio, G.R., Lardone, R.D., Le, D., Varki, N.M., Nizet, V., and Marth, J.D. (2013). Inducing host protection in pneumococcal sepsis by preactivation of the Ashwell-Morell receptor. Proc. Natl. Acad. Sci. USA *110*, 20218–20223.

Hartman, M.E., Linde-Zwirble, W.T., Angus, D.C., and Watson, R.S. (2013). Trends in the epidemiology of pediatric severe sepsis. Pediatr. Crit. Care Med. *14*, 686–693.

Hata, K., Koseki, K., Yamaguchi, K., Moriya, S., Suzuki, Y., Yingsakmongkon, S., Hirai, G., Sodeoka, M., von Itzstein, M., and Miyagi, T. (2008). Limited inhibitory effects of oseltamivir and zanamivir on human sialidases. Antimicrob. Agents Chemother. *52*, 3484–3491.

Hawiger, J., and Musser, J.M. (2011). How to approach genome wars in sepsis? Crit. Care *15*, 1007.

Heemskerk, S., Masereeuw, R., Moesker, O., Bouw, M.P., van der Hoeven, J.G., Peters, W.H., Russel, F.G., and Pickkers, P.; APSEP Study Group (2009). Alkaline phosphatase treatment improves renal function in severe sepsis or septic shock patients. Crit. Care Med. *37*, 417–423, e1.

Heithoff, D.M., Shimp, W.R., House, J.K., Xie, Y., Weimer, B.C., Sinsheimer, R.L., and Mahan, M.J. (2012). Intraspecies variation in the emergence of hyperinfectious bacterial strains in nature. PLoS Pathog. *8*, e1002647.

Ishibashi, S., Hammer, R.E., and Herz, J. (1994). Asialoglycoprotein receptor deficiency in mice lacking the minor receptor subunit. J. Biol. Chem. *269*, 27803–27806.

Iwashyna, T.J., Ely, E.W., Smith, D.M., and Langa, K.M. (2010). Long-term cognitive impairment and functional disability among survivors of severe sepsis. JAMA *304*, 1787–1794.

Kats, S., Brands, R., Seinen, W., de Jager, W., Bekker, M.W., Hamad, M.A., Tan, M.E., and Schönberger, J.P. (2009). Anti-inflammatory effects of alkaline phosphatase in coronary artery bypass surgery with cardiopulmonary bypass. Recent Pat. Inflamm. Allergy Drug Discov. *3*, 214–220.

Kiffer-Moreira, T., Sheen, C.R., Gasque, K.C., Bolean, M., Ciancaglini, P., van Elsas, A., Hoylaerts, M.F., and Millán, J.L. (2014). Catalytic signature of a heat-stable, chimeric human alkaline phosphatase with therapeutic potential. PLoS One *9*, e89374.

Koyama, I., Matsunaga, T., Harada, T., Hokari, S., and Komoda, T. (2002). Alkaline phosphatases reduce toxicity of lipopolysaccharides in vivo and in vitro through dephosphorylation. Clin. Biochem. *35*, 455–461.

Lee, C.H., and Tsai, C.M. (1999). Quantification of bacterial lipopolysaccharides by the purpald assay: measuring formaldehyde generated from 2-keto-3-deoxyoctonate and heptose at the inner core by periodate oxidation. Anal. Biochem. *267*, 161–168.

Lin, J.N., Lai, C.H., Chen, Y.H., Chang, L.L., Lu, P.L., Tsai, S.S., Lin, H.L., and Lin, H.H. (2010). Characteristics and outcomes of polymicrobial bloodstream infections in the emergency department: A matched case-control study. Acad. Emerg. Med. *17*, 1072–1079.

Lukas, M., Drastich, P., Konecny, M., Gionchetti, P., Urban, O., Cantoni, F., Bortlik, M., Duricova, D., and Bulitta, M. (2010). Exogenous alkaline phosphatase for the treatment of patients with moderate to severe ulcerative colitis. Inflamm. Bowel Dis. *16*, 1180–1186.

Marshall, J.C. (2014). Why have clinical trials in sepsis failed? Trends Mol. Med. *20*, 195–203.

Millán, J.L. (2006). Mammalian Alkaline Phosphatases: From Biology to Applications in Medicine and Biotechnology (Weinheim, Chichester: Wiley-VCH).

Narisawa, S., Fröhlander, N., and Millán, J.L. (1997). Inactivation of two mouse alkaline phosphatase genes and establishment of a model of infantile hypophosphatasia. Dev. Dyn. *208*, 432–446.

Narisawa, S., Huang, L., Iwasaki, A., Hasegawa, H., Alpers, D.H., and Millán, J.L. (2003). Accelerated fat absorption in intestinal alkaline phosphatase knockout mice. Mol. Cell. Biol. *23*, 7525–7530.

Ohtsubo, K., Chen, M.Z., Olefsky, J.M.A., and Marth, J.D. (2011). Pathway to diabetes through attenuation of pancreatic beta cell glycosylation and glucose transport. Nat. Med. *17*, 1067–1075.

Opal, S.M., Laterre, P.F., Francois, B., LaRosa, S.P., Angus, D.C., Mira, J.P., Wittebole, X., Dugernier, T., Perrotin, D., Tidswell, M., et al.; ACCESS Study Group (2013). Effect of eritoran, an antagonist of MD2-TLR4, on mortality in patients with severe sepsis: the ACCESS randomized trial. JAMA *309*, 1154–1162.

Orban, J.C., Walrave, Y., Mongardon, N., Allaouchiche, B., Argaud, L., Aubrun, F., Barjon, G., Constantin, J.M., Dhonneur, G., Durand-Gasselin, J., et al.; AzuRéa Network (2017). Causes and Characteristics of Death in Intensive Care Units: A Prospective Multicenter Study. Anesthesiology *126*, 882–889.

Pammi, M., Zhong, D., Johnson, Y., Revell, P., and Versalovic, J. (2014). Polymicrobial bloodstream infections in the neonatal intensive care unit are associated with increased mortality: a case-control study. BMC Infect. Dis. *14*, 390.

Park, B.S., Song, D.H., Kim, H.M., Choi, B.S., Lee, H., and Lee, J.O. (2009). The structural basis of lipopolysaccharide recognition by the TLR4-MD-2 complex. Nature *458*, 1191–1195.

Parlato, M., Charbit-Henrion, F., Pan, J., Romano, C., Duclaux-Loras, R., Le Du, M.H., Warner, N., Francalanci, P., Bruneau, J., Bras, M., et al. (2018). Human ALPI deficiency causes inflammatory bowel disease and highlights a key mechanism of gut homeostasis. EMBO Mol. Med. *10*, e8483.

Peters, E., Stevens, J., Arend, J., Guan, Z., Raaben, W., Laverman, P., Elsas, A.V., Masereeuw, R., and Pickkers, P. (2015). Biodistribution and translational pharmacokinetic modeling of a human recombinant alkaline phosphatase. Int. J. Pharm. *495*, 122–131.

Pettengill, M., Matute, J.D., Tresenriter, M., Hibbert, J., Burgner, D., Richmond, P., Millán, J.L., Ozonoff, A., Strunk, T., Currie, A., and Levy, O. (2017). Human alkaline phosphatase dephosphorylates microbial products and is elevated in preterm neonates with a history of late-onset sepsis. PLoS One *12*, e0175936.

Pickkers, P., Heemskerk, S., Schouten, J., Laterre, P.F., Vincent, J.L., Beishuizen, A., Jorens, P.G., Spapen, H., Bulitta, M., Peters, W.H., and van der Hoeven, J.G. (2012). Alkaline phosphatase for treatment of sepsis-induced acute kidney injury: a prospective randomized double-blind placebo-controlled trial. Crit. Care *16*, R14.

Pinkerton, A.B., Sergienko, E., Bravo, Y., Dahl, R., Ma, C.T., Sun, Q., Jackson, M.R., Cosford, N.D.P., and Millán, J.L. (2018). Discovery of 5-((5-chloro-2-methoxyphenyl)sulfonamido)nicotinamide (SBI-425), a potent and orally bioavailable tissue-nonspecific alkaline phosphatase (TNAP) inhibitor. Bioorg. Med. Chem. Lett. *28*, 31–34.

Poelstra, K., Bakker, W.W., Klok, P.A., Hardonk, M.J., and Meijer, D.K. (1997). A physiologic function for alkaline phosphatase: endotoxin detoxification. Lab. Invest. *76*, 319–327.

Poltorak, A., He, X., Smirnova, I., Liu, M.Y., Van Huffel, C., Du, X., Birdwell, D., Alejos, E., Silva, M., Galanos, C., et al. (1998). Defective LPS signaling in C3H/HeJ and C57BL/10ScCr mice: mutations in Tlr4 gene. Science *282*, 2085–2088.

Poolman, J.T., and Wacker, M. (2016). Extraintestinal pathogenic Escherichia coli, a common human pathogen: challenges for vaccine development and progress in the field. J. Infect. Dis. *213*, 6–13.

Rice, T.W., Wheeler, A.P., Bernard, G.R., Vincent, J.L., Angus, D.C., Aikawa, N., Demeyer, I., Sainati, S., Amlot, N., Cao, C., et al. (2010). A randomized, double-blind, placebo-controlled trial of TAK-242 for the treatment of severe sepsis. Crit. Care Med. *38*, 1685–1694.

Russo, T.A., Thompson, J.S., Godoy, V.G., and Malamy, M.H. (1990). Cloning and expression of the Bacteroides fragilis TAL2480 neuraminidase gene, nanH, in Escherichia coli. J. Bacteriol. *172*, 2594–2600.

Schromm, A.B., Brandenburg, K., Loppnow, H., Zähringer, U., Rietschel, E.T., Carroll, S.F., Koch, M.H., Kusumoto, S., and Seydel, U. (1998). The charge of endotoxin molecules influences their conformation and IL-6-inducing capacity. J. Immunol. *161*, 5464–5471.

Schulte, W., Bernhagen, J., and Bucala, R. (2013). Cytokines in sepsis: potent immunoregulators and potential therapeutic targets–an updated view. Mediators Inflamm. *2013*, 165974.

Sheen, C.R., Kuss, P., Narisawa, S., Yadav, M.C., Nigro, J., Wang, W., Chhea, T.N., Sergienko, E.A., Kapoor, K., Jackson, M.R., et al. (2015). Pathophysiological role of vascular smooth muscle alkaline phosphatase in medial artery calcification. J. Bone Miner. Res. *30*, 824–836.

Singleton, K.D., and Wischmeyer, P.E. (2003). Distance of cecum ligated influences mortality, tumor necrosis factor-alpha and interleukin-6 expression following cecal ligation and puncture in the rat. Eur. Surg. Res. *35*, 486–491.

Soukharev, S., Miller, J.L., and Sauer, B. (1999). Segmental genomic replacement in embryonic stem cells by double lox targeting. Nucleic Acids Res. *27*, e21.

Stearns-Kurosawa, D.J., Osuchowski, M.F., Valentine, C., Kurosawa, S., and Remick, D.G. (2011). The pathogenesis of sepsis. Annu. Rev. Pathol. *6*, 19–48.

Stevenson, E.K., Rubenstein, A.R., Radin, G.T., Wiener, R.S., and Walkey, A.J. (2014). Two decades of mortality trends among patients with severe sepsis: a comparative meta-analysis. Crit. Care Med. *42*, 625–631.

Takao, K., and Miyakawa, T. (2015). Genomic responses in mouse models greatly mimic human inflammatory diseases. Proc. Natl. Acad. Sci. USA *112*, 1167–1172.

Tuin, A., Huizinga-Van der Vlag, A., van Loenen-Weemaes, A.M., Meijer, D.K., and Poelstra, K. (2006). On the role and fate of LPS-dephosphorylating activity in the rat liver. Am. J. Physiol. Gastrointest. Liver Physiol. *290*, G377–G385.

van Sorge, N.M., Beasley, F.C., Gusarov, I., Gonzalez, D.J., von Köckritz-Blickwede, M., Anik, S., Borkowski, A.W., Dorrestein, P.C., Nudler, E., and Nizet, V. (2013). Methicillin-resistant Staphylococcus aureus bacterial nitric-oxide synthase affects antibiotic sensitivity and skin abscess development. J. Biol. Chem. *288*, 6417–6426.

Vimr, E.R., and Troy, F.A. (1985). Identification of an inducible catabolic system for sialic acids (nan) in Escherichia coli. J. Bacteriol. *164*, 845–853.

Vincent, J.L., Martinez, E.O., and Silva, E. (2009). Evolving concepts in sepsis definitions. Crit. Care Clin. *25*, 665–675, vii.

Yang, W.H., Nussbaum, C., Grewal, P.K., Marth, J.D., and Sperandio, M. (2012). Coordinated roles of ST3Gal-VI and ST3Gal-IV sialyltransferases in the synthesis of selectin ligands. Blood *120*, 1015–1026.

Yang, W.H., Aziz, P.V., Heithoff, D.M., Mahan, M.J., Smith, J.W., and Marth, J.D. (2015). An intrinsic mechanism of secreted protein aging and turnover. Proc. Natl. Acad. Sci. USA *112*, 13657–13662.

Yang, W.H., Heithoff, D.M., Aziz, P.V., Sperandio, M., Nizet, V., Mahan, M.J., and Marth, J.D. (2017). Recurrent infection progressively disables host protection against intestinal inflammation. Science *358*, eaao5610.

STAR★METHODS

KEY RESOURCES TABLE

REAGENT or RESOURCE	SOURCE	IDENTIFIER
Antibodies		
Goat polyclonal anti-TNAP	Santa Cruz Biotechnology	Cat #: sc-23430; RRID: AB_667751
Rabbit polyclonal anti-TNAP	Abcam	Cat #: ab65834; RRID: AB_1139987
Rabbit polyclonal IAP-specific antiserum	Narisawa et al., 2003	N/A
Rabbit polyclonal Neu1 antibody	Santa Cruz Biotechnology	Cat #: sc-32936; RRID: AB_2298197
Goat polyclonal Neu2 antibody	Santa Cruz Biotechnology	Cat #: sc-168736; RRID: AB_10840952
Rabbit polyclonal Neu3 antibody	Santa Cruz Biotechnology	Cat #: sc-134931; RRID: AB_10609640
Goat polyclonal Neu4 antibody	Santa Cruz Biotechnology	Cat #: sc-161127; RRID: AB_2149077
Goat polyclonal ASGR1 antibody	Santa Cruz Biotechnology	Cat #: sc-13469; RRID: AB_2059810
Goat polyclonal ASGR2 antibody	Santa Cruz Biotechnology	Cat #: sc-13471; RRID: AB_2059821
FITC-conjugated goat anti-rabbit IgG	Santa Cruz Biotechnology	Cat #: sc-2090; RRID: AB_641179
Texas Red-conjugated rabbit anti-goat IgG	Santa Cruz Biotechnology	Cat #: sc-3919; RRID: AB_654579
Bacterial and Virus Strains		
Salmonella enterica serovar Typhimurium	CDC 6516-60	ATCC 14028
Escherichia coli	FDA strain Seattle 1946	ATCC 25922
Streptococcus pneumoniae	Serotype 2 strain D39	N/A
Staphylococcus aureus, methicillin-resistant	CA-MRSA USA300	N/A
Staphylococcus aureus, methicillin-sensitive	Newman	N/A
Chemicals, Peptides, and Recombinant Proteins		
HRP-conjugated *Erythrina cristagalli* lectin	EY Laboratories	Cat #: H-5901-1
HRP-conjugated *Ricinus Communis Agglutinin*-I lectin	EY Laboratories	Cat #: H-2001-1
HRP-conjugated Peanut Agglutinin lectin	EY Laboratories	Cat #: H-2301-1
HRP-conjugated *Maackia amurensis*-II lectin	EY Laboratories	Cat #: H-7801-1
HRP-conjugated *Sambucus nigra* lectin	EY Laboratories	Cat #: H-6802-1
Calf intestinal alkaline phosphatase	Lee Biosolutions	Cat #: 480-20
Calf intestinal alkaline phosphatase	Invitrogen	Cat #: 18009019
Amersham ECL Western Blotting Detection Reagent	GE Healthcare	Cat #: RPN2109
Coomassie brilliant blue G250	Bio-Rad	Cat #: 1610406
N-hydroxysuccinimide-biotin	Thermo Fisher Scientific	Cat #: 21338
HRP-conjugated streptavidin	BD Biosciences	Cat #: 554066
3,3′,5,5′-Tetramethylbenzidine (TMB) Liquid Substrate	Sigma-Aldrich	Cat #: T0440
Proteinase K	Promega	Cat #: V3021
RNase A	Invitrogen	Cat #: 12091021
DNase I	Invitrogen	***Cat #: 18047019***
Purpald	Sigma-Aldrich	Cat #: 162892
Sodium periodate	Sigma-Aldrich	Cat #: 210048
Silver stain plus	Bio-Rad	Cat #: 1610449
p-nitrophenylphosphate (pNPP) alkaline phosphatase liquid substrate	Sigma-Aldrich	Cat #: P7998
Pierce monomeric avidin kit	Thermo Fisher Scientific	Cat #: 20227
2,3-dehydro-2-deoxy-*N*-acetylneuraminic acid	Calbiochem	Cat #: 252926
Zanamivir	Sigma-Aldrich	Cat #: SML0492
E. coli O111:B4 LPS	Sigma-Aldrich	Cat #: L4391
TRIzol	Invitrogen	Cat #: 15596026
10% buffered formalin	Sigma-Aldrich	Cat #: HT5014
Tissue-Tek OCT compound, Sakura Finetek	VWR	Cat #: 25608-930

(*Continued on next page*)

Continued

REAGENT or RESOURCE	SOURCE	IDENTIFIER
Mayer's hematoxylin solution	Sigma-Aldrich	Cat #: MHS16
Eosin Y solution	Sigma-Aldrich	Cat #: HT110116
Neuraminidase (from *Arthrobacter ureafaciens*)	EY Laboratories	Cat #: EC-32118-5
SBI-425, TNAP inhibitor	Sheen et al., 2015	N/A
Critical Commercial Assays		
VetScan Comprehensive Diagnostic Profile reagent rotor	Abaxis	Cat #: 500-0038
IL-1 beta mouse ELISA kit	Thermo Fisher Scientific	Cat #: KMC0011
IL-6 beta mouse ELISA kit	Thermo Fisher Scientific	Cat #: KMC0061
IFN gamma mouse ELISA kit	Thermo Fisher Scientific	Cat #: KMC4021
TNF alpha mouse ELISA kit	Thermo Fisher Scientific	Cat #: KMC3011
Malachite Green Phosphate Assay Kit	BioAssay Systems	Cat #: POMG-25H
Amplex Red Neuraminidase Assay Kit	Thermo Fisher Scientific	Cat #: A22178
NA-XTD Neuraminidase Assay Kit	Applied Biosystems	Cat #: 4457535
SuperScript III reverse transcriptase kit	Invitrogen	Cat #: 18080093
Brilliant SYBR green qPCR master mix kit	Agilent Technologies	Cat #: 600830
Experimental Models: Organisms/Strains		
Asgr1$^{-/-}$ mice	Soukharev et al., 1999	N/A
Asgr2$^{-/-}$ mice	Ishibashi et al., 1994	N/A
St3gal6$^{\Delta/\Delta}$ mice	Yang et al., 2012	N/A
Akp3$^{-/-}$ mice	Narisawa et al., 2003	N/A
Tlr4$^{-/-}$ mice (B6(Cg)-Tlr4$^{tm1.2Karp}$/J)	The Jackson Laboratory	Stock #: 029015
St3gal6$^{\Delta/\Delta}$ *Asgr1*$^{-/-}$ mice	This study	N/A
St3gal6$^{\Delta/\Delta}$ *Asgr1*$^{-/-}$ mice	This study	N/A
Oligonucleotides		
TNAP-forward: CCCAGACACAAGCATTCCCACTAT	Yang et al., 2015	N/A
TNAP-reverse: CACCATCTCGGAGAGCG	Yang et al., 2015	N/A
IAP-forward: CTCATCTCCAACATGGAC	Yang et al., 2015	N/A
IAP-reverse: TGCTTAGCACTTTCACGG	Yang et al., 2015	N/A
GAPDH -forward: TGGTGAAGGTCGGTGTGAAC	Yang et al., 2015	N/A
GAPDH -reverse: AGTGATGGCATGGACTGTGG	Yang et al., 2015	N/A
Software and Algorithms		
GraphPad Prism 7.0	GraphPad Software	https://www.graphpad.com/scientific-software/prism/
Microsoft Excel	Microsoft	https://products.office.com/en-us/excel
TissueFAXS imaging software 3.5	TissueGnostics imaging solution	http://www.tissuegnostics.com/en/products/imaging-software/170-tissuefaxs-imaging-software
TissueQuest Analysis software 4.0	TissueGnostics imaging solution	http://www.tissuegnostics.com/en/products/analysing-software/tissuequest
HistoQuest Analysis software 4.0	TissueGnostics imaging solution	http://www.tissuegnostics.com/en/products/analysing-software/histoquest

CONTACT FOR REAGENT AND RESOURCE SHARING

Further information and requests for resources and reagents should be directed to and will be fulfilled by the Lead Contact, Jamey D. Marth (jmarth@sbpdiscovery.org).

EXPERIMENTAL MODEL AND SUBJECT DETAILS

Laboratory Animals

Animal experiments were carried out with adult 8–12-week-old mice and used equal numbers of male and female mice. All mice analyzed were provided sterile pellet food and water *ad libitum*. Institutional Animal Care and Use Committees of the University of

California Santa Barbara and the Sanford-Burnham-Prebys Medical Discovery Institute approved studies undertaken herein. All mice were housed with their littermates in groups of four or five animals per cage in a specific pathogen-free barrier facility at the University of California Santa Barbara.

Mice bearing null alleles of *Asgr1, Asgr2, and Akp3* have been previously described (Ishibashi et al., 1994; Narisawa et al., 2003; Soukharev et al., 1999). *St3gal6*-deficient mice have been previously described (Yang et al., 2012). We generated mice homozygous for multiple mutant alleles including *St3gal6*$^{\Delta/\Delta}$ *Asgr1*$^{-/-}$ or *St3gal6*$^{\Delta/\Delta}$ *Asgr2*$^{-/-}$. *Tlr4*$^{-/-}$ mice (B6(Cg)-Tlr4$^{tm1.2Karp}$/J) were purchased from Jackson Laboratory. All strains of mice were backcrossed six or more generations into the C57BL/6J background prior to study. Animals bearing multiple mutations for study were generated from compound heterozygote mates to produce offspring bearing both control and experimental genotypes. Littermates bearing normal alleles were used as controls. No statistical methods were used to pre-determine sample sizes; sample sizes were determined based on previous studies (Grewal et al., 2008 and 2013).

Bacterial Strains and Culture Conditions

Escherichia coli (EC) strain ATCC 25922 (clinical isolate, FDA strain Seattle 1946), *Salmonella* enterica serovar Typhimurium (*ST*) reference strain ATCC 14028 (CDC 6516-60), *Streptococcus pneumoniae* (*SPN)* serotype 2 strain D39, methicillin-resistant *Staphylococcus aureus* (*MRSA*) strain CA-MRSA USA300 and methicillin-sensitive *Staphylococcus aureus* (*MSSA*) strain Newman were used as previously described (Beumer et al., 2003; Chow et al., 2010; Grewal et al., 2008; Heithoff et al., 2012; van Sorge et al., 2013).

EC, MRSA, and MSSA were streaked from frozen stocks onto Tryptic Soy (TS) agar plates and incubated overnight at 37°C. Single colonies were inoculated into TS broth and incubated overnight with shaking at 37°C. After overnight incubation, *MRSA* and *MSSA* were re-inoculated as 1:100 sub-cultures into fresh TS broth and cultured to mid-log phase (A_{600} = 0.4). *EC, MRSA, and MSSA* were pelleted by centrifugation, washed, and suspended in sterile PBS.

ST was streaked from frozen stocks onto Luria-Bertani (LB) agar plates and incubated overnight at 37°C. Single colonies were inoculated into LB broth and incubated overnight with shaking at 37°C. *ST* was pelleted by centrifugation, washed, and suspended in sterile 0.2M sodium phosphate buffer (pH 8.1).

SPN was streaked from frozen stocks onto Todd-Hewitt (TH) agar plates containing 2% yeast extract and incubated overnight at 37°C in a 5% CO_2 incubator. Single colonies were inoculated into TH broth containing 2% yeast extract and incubated overnight with shaking at 37°C in a 5% CO_2 incubator. After overnight incubation, *SPN* was re-inoculated as a 1:10 sub-culture into fresh TH broth and cultured to mid-log phase (A_{600} = 0.4). *SPN* was pelleted by centrifugation, washed, and suspended in sterile PBS.

METHOD DETAILS

Bacterial Infections

EC and *SPN* were administered i.p.; *EC* at a dose of 1 × 10^7 *cf.*u (10X LD_{50}) and *SPN* at a dose of 1 × 10^4 *cf.*u (10X LD_{50}); *ST* was administered via gastric intubation at a dose of 1 × 10^7 *cf.*u (20X LD_{50}), or i.p. at a dose of 1 × 10^3 *cf.*u (20X LD_{50}); *MRSA* and *MSSA* were administered i.v.; *MRSA* at a dose of 1 × 10^8 *cf.*u (20X LD_{50}) and *MSSA* at a dose of 5 × 10^8 *cf.*u (20X LD_{50}). LD_{50} values were determined by identifying the inoculum dose that resulted in death of 50% infected animals following delivery of pathogen by indicated route of infection. Blood was collected to enumerate bacterial *cf.*u at the indicated times after infection, and mice with equivalent bacteremia (between 1 × 10^2 *cf.*u/mL and 1 × 10^4 *cf.*u/mL at 24 h after *EC* infection, 1 × 10^1 *cf.*u/mL and 1 × 10^3 *cf.*u/mL at day 5 after *ST* gastric intubation infection, 1 × 10^1 *cf.*u/mL and 1 × 10^3 *cf.*u/mL at 48 h after *ST* i.p. infection, or 1 × 10^3 *cf.*u/mL and 1 × 10^5 *cf.*u/mL at 24 h after *SPN*, *MRSA* or *MSSA* infection followed by an increase to between 1 × 10^4 *cf.*u/mL and 1 × 10^6 *cf.*u/mL at 48 h after *EC* infection, 1 × 10^3 *cf.*u/mL and 1 × 10^6 *cf.*u/mL at day 8 after *ST* gastric intubation infection, 1 × 10^3 *cf.*u/mL and 1 × 10^6 *cf.*u/mL at day 5 after *ST* i.p. infection, or 1 × 10^5 *cf.*u/mL and 1 × 10^7 *cf.*u/mL at 48 h after *SPN*, *MRSA* or *MSSA* infection) were studied further. Using this protocol, blood *cf.*u from approximately 60% of *EC*-infected mice, approximately 20% of *ST*-infected mice (gastric intubation or i.p. delivery), and approximately 50% of *SPN*, *MRSA*, or *MSSA*-infected mice were outside the target blood *cf.*u/mL range. Mice and their blood samples outside of the target range were not analyzed further. Mouse morbidity and survival were plotted with Kaplan Meier analyses generated using Graphpad Prism software.

Blood Chemistry and Calf Intestinal Alkaline Phosphatase Treatment

Blood was collected from anesthetized animals into Microtainer Serum Separator Tubes (BD Biosciences) with no anticoagulant and allowed to clot for 30 min at room temperature. Serum was collected after centrifugation at 13,000 rpm for 10 min. Serum chemistry values including measurements of albumin, alkaline phosphatase activity, alanine transferase activity, amylase activity, total bilirubin, blood urea nitrogen, calcium, phosphorus, creatinine, glucose, sodium, potassium, total protein, and globulin were acquired with a VetScan Comprehensive Diagnostic Profile reagent rotor using the VetScan Chemistry Analyzer as previously reported (Grewal et al., 2013; Yang et al., 2015). AP activity measured in serum from wild-type uninfected C57BL/6J mice serum was 113.1 ± 4.3 U/L as the mean ± SEM (n = 30). Calf intestinal alkaline phosphatase (cIAP) (Lee Biosolutions) was i.v. administered at 75 U/kg in 200 μl of PBS (Beumer et al., 2003).

Glycoprotein Immunoprecipitation, Western Blotting, and Lectin Blotting

Serum samples diluted in RIPA buffer (50 mM Tris-HCl (pH 7.6), 150 mM NaCl, 1 mM EDTA, 1% NP-40, 1% sodium deoxycholate and 0.1% SDS) were supplemented with complete protease inhibitor cocktail per instructions (Roche) and incubated overnight at 4°C on a rotating wheel with either 2 μg/mL of TNAP antibody (N-18; Santa Cruz Biotechnology), or 1:100 dilution of IAP-specific antiserum (Narisawa et al., 2003) followed by 2 h of incubation in the presence of protein A/G PLUS-agarose (Santa Cruz Biotechnology). Immunoprecipitates were washed five times with RIPA buffer and eluted with SDS sample buffer for SDS-PAGE. Protein samples eluted were subjected to SDS-PAGE, transferred to nitrocellulose membranes and incubated with 2% BSA in Tris-buffered saline (TBS). They were then analyzed by western blotting using 1 μg/mL of anti-TNAP antibody (ab65834; Abcam), 1 μg/mL of anti-Neu1 (H-300; Santa Cruz Biotechnology), anti-Neu2 (M-13; Santa Cruz Biotechnology), anti-Neu3 (M-50; Santa Cruz Biotechnology), anti-Neu4 (N-14; Santa Cruz Biotechnology), or 1:1000 dilution of anti-IAP antiserum, or by lectin blotting with HRP-conjugated *Erythrina cristagalli* (ECA, 0.5 μg/mL), *Ricinus Communis Agglutinin*-I (RCA, 0.1 μg/mL), Peanut Agglutinin (PNA, 1 μg/mL), *Maackia amurensis*-II (MAL-II, 0.2 μg/mL), or *Sambucus nigra* (SNA, 0.1 μg/mL) (EY Laboratories). Signals detected by chemiluminescence (GE Healthcare) were analyzed by integrated optical density using Labworks software (UVP Bioimaging Systems). Parallel protein samples were visualized with Coomassie brilliant blue G250 staining (Bio-Rad).

Enzyme-Linked Immunosorbent Assay and Serum Cytokine Measurements

Enzyme-linked immunosorbent assay (ELISA) plates (Nunc) were coated with antibodies to either TNAP (N-18), Neu1 (H-300), Neu2 (M-13), Neu3 (M-50), or Neu4 antibody (N-14), or IAP antiserum, and blocked with BSA before incubation with serial dilutions of mouse serum samples that were biotinylated using 1 mg/mL of *N*-hydroxysuccinimide-biotin (Thermo Fisher Scientific). Antigens were detected following the addition of HRP-streptavidin (BD Biosciences) and 3,3′,5,5′ tetramethylbenzidine (TMB; Sigma-Aldrich). Lectin binding was determined in parallel by the addition of HRP-conjugated ECA, RCA, PNA, MAL-II or SNA, followed by TMB, and changes in glycan linkages were detected by comparing lectin binding among identical amounts of biotinylated TNAP and IAP antigen calculated as described (Ellies et al., 2002). Cytokine ELISA assays including IL-1β (KMC0011; Thermo Fisher Scientific), IL-6 (KMC0061; Thermo Fisher Scientific), IFN-γ (KMC4021; Thermo Fisher Scientific) and TNF-α (KMC3011; Thermo Fisher Scientific) were performed according to the manufacturers' instructions.

LPS Phosphorylation

To determine LPS content in mouse serum, LPS was isolated as previously described (Davis and Goldberg, 2012) by the hot phenol-water method with minor modifications. Briefly, blood was collected into Microtainer Serum Separator Tubes. 0.5 mL of serum was added to 0.5 mL of 99% phenol (Ambion) preheated to 65°C and incubated for 15 min at 65°C. After cooling on ice, the samples were centrifuged at 13,000 rpm for 10 min. The aqueous phase was acquired and residual phenol was removed by extracting with diethyl ether (Sigma-Aldrich). The diethyl ether phase was discarded and the water phase containing the LPS was placed in a hood for 1 h to allow the remaining diethyl ether to evaporate. The above steps were repeated after treatment with proteinase K (Promega), RNase (Invitrogen) and DNase (Invitrogen). Sodium acetate at 0.5 M final concentration and 10 volumes of 95% ethanol were added and the samples were stored at –20°C overnight in order to precipitate LPS. The samples were centrifuged at 13,000 rpm for 10 min and the pellets were resuspended in distilled water. LPS preparations from indicated sources were quantified by the purpald assay as described previously (Lee and Tsai, 1999). LPS preparations for comparative studies were indistinguishable by chromatography and silver staining (Bio-Rad). To compare the abundance of phosphate linked to LPS, phosphate release was measured by the malachite green phosphate assay (Goldberg et al., 2008). Briefly, purified calf intestinal alkaline phosphatase (10 U; Invitrogen) was incubated at pH 8.0 for 3 h at 37°C with 1 μg of LPS isolated from mouse serum. Free phosphate released was measured as a colored complex of phosphomolybdate and malachite green at 620 nm according to the manufacturers' instructions (BioAssay Systems).

Blood Glycoprotein Half-Life

N-hydroxysuccinimide-biotin (10 mg/kg of mouse body weight; Pierce) was i.v. injected into adult mice (Grewal et al., 2008). Subsequently, whole blood was collected at the indicated times into Microtainer Serum Separator Tubes (BD Biosciences) by tail bleeds of anesthetized mice. Biotinylated serum glycoproteins were isolated by affinity chromatography using immobilized monomeric avidin gel and eluted in the presence of D-biotin (Pierce). Time 0 was defined as 1 h after reactive biotin injection, when biotinylation stopped and proteins were maximally biotinylated (100% relative biotinylation). Biotinylated serum TNAP and IAP were captured on ELISA plates coated with anti-TNAP antibody or IAP antiserum. TNAP and IAP protein levels were quantified following administration of detection reagents HRP-streptavidin and TMB.

Neuraminidase Activity and Inhibition

Neuraminidase activity was measured in total serum obtained from blood isolated from either the tail vein or by cardiac puncture. The Amplex Red neuraminidase assay was used according to the manufacturers' instructions (Thermo Fisher Scientific). In brief, 5 μl of freshly prepared serum samples obtained from tail bleeds were added to 45 μl of the Amplex Red reaction buffer and mixed with 50 μl of the Amplex Red working solution. The mixtures were incubated for 30 min at 37°C and absorbance was measured at 560 nm. In addition, fluorescence of the mixtures was measured using excitation at 530 nm and emission detection at 590 nm. Specific neuraminidase activity was calculated using a standard of *Arthrobacter ureafaciens* neuraminidase (EY Laboratories) serially diluted

2-fold in PBS starting at 500 U/L. Serum neuraminidase activity measured among uninfected wild-type C57BL/6J mice (8-12 weeks old) using the Amplex Red assay was 85.0 ± 4.5 U/L as the mean ± SEM (n = 20).

A direct assay of neuraminidase activity was adapted from the NA-XTD assay (Applied Biosystems) and was used to compare selected data obtained using the Amplex Red assay. The NA-XTD assay was used according to manufacturer's instructions with the following exceptions: 5 μl of freshly prepared serum obtained from cardiac puncture was used, 26 mM MES (2-(N-morpholino) ethanesulfonic acid) buffer was supplemented with 4 mM $CaCl_2$ at pH 7.4, and reaction was incubated for 30 min at 37°C. Results obtained using the NA-XTD assay confirmed the relative changes of neuraminidase activity detected using the Amplex Red assay; however, the basal Neu activity measured among uninfected wild-type C57BL/6J mice using the NA-XTD assay was 44.4 ± 10.0 mU/L as the mean ± SEM (n = 6). Specific units were derived from standard curves using *Arthrobacter ureafaciens* neuraminidase (EY Laboratories) serially diluted 2-fold in PBS starting at 500 mU/L.

Inhibition of serum neuraminidase activity was achieved as presented using 250 mg/kg of either 2,3-dehydro-2-deoxy-*N*-acetylneuraminic acid (DANA; Calbiochem) (Cross et al., 2012) or Zanamivir (Sigma-Aldrich) (Hata et al., 2008) was prepared in 200 μl of PBS and injected intravenously (i.v.) following infection and at multiple time points (every 24 h) (Yang et al., 2015).

TNAP Inhibition

SBI-425, a selective inhibitor of TNAP activity, was injected into the intraperitoneal cavity at a dose of 10 mg/kg in 200 μl of the dosing vehicle consisting of 10% DMSO, 10% Tween-20, and 80% water (Sheen et al., 2015).

LPS-induced Toxicity

Mice were i.p. injected with *E. coli* O111:B4 LPS (Sigma-Aldrich) and Kaplan Meier survival graphs were generated in Graphpad Prism software.

mRNA Analyses

Total RNA was isolated from tissues using Trizol (Invitrogen) and subjected to reverse transcription (RT) using SuperScript III (Invitrogen). Quantitative real-time PCR was performed using Brilliant SYBR Green Reagents (Agilent Technologies) with the Mx3000P QPCR System (Stratagene). Primers used for real-time PCR in the mouse were: TNAP-RT-forward (F) (5′-CCCAGACA CAAGCATTCCCACTAT-3′), TNAP-RT-reverse (R) (5′-CACCATCTCGGAGAGCG-3′), IAP-RT-F (5′- CTCATCTCCAACATGGAC-3′), IAP-RT-R (5′-TGCTTAGCACTTTCACGG-3′), GAPDH-RT-F (5′-TGGTGAAGGTCGGTGTGAAC-3′) and GAPDH-RT-R (5′-AGT GATGGCATGGACTGTGG-3′). Relative mRNA levels were normalized to littermate WT control expression of GAPDH RNA.

Histology

Mouse liver tissues were fixed in 10% buffered formalin (Sigma-Aldrich), transferred to 30% sucrose/PBS, and embedded in Tissue-Tek OCT compound (Sakura Finetek). For immunofluorescence analysis, 5 μm frozen serial sections were incubated with anti-TNAP antibody (ab65834; Abcam) or IAP antiserum combined with either ASGR1 antibody (T-20; Santa Cruz Biotechnology) or ASGR2 antibody (N-17; Santa Cruz Biotechnology). TNAP and IAP were visualized with FITC-conjugated goat anti-rabbit IgG (Santa Cruz Biotechnology) and ASGR1 and ASGR2 were visualized with Texas Red-conjugated rabbit anti-goat IgG (Santa Cruz Biotechnology). These primary antibody incubations (1:200 dilutions) were performed at 4°C overnight and secondary antibody incubations (1:1000 dilution) were performed at room temperature for 1 h. Serial sections were stained with hematoxylin and eosin (H&E; Sigma-Aldrich). Immunofluorescence images were obtained and analyzed using a TissueGnostics microscopy workstation with TissueFAXS, TissueQuest, and HistoQuest software (TissueGnostics USA Ltd.) (Ohtsubo et al., 2011).

Experimental Design

For all studies, at least 6 animals per experimental group were used and all experiments were conducted in at least duplicate with similar results. No statistical methods were used to pre-determine sample sizes, but our sample sizes were determined based on previous studies (Grewal et al., 2008,2013). All animal experiments were conducted with inbred C57BL/6J mice which according to their genetic homology were not randomly allocated to experimental groups. We were not blinded to the group allocation.

QUANTIFICATION AND STATISTICAL ANALYSIS

All experiments were performed a minimum of two independent replications. Data were analyzed as mean ± SEM unless otherwise indicated. All data meet the assumptions of the tests. Student's unpaired t test was used to compare the means of two groups. One-way Analysis of Variance (ANOVA) with Tukey's multiple comparisons test was used to compute statistical significance between multiple groups. Log-rank test was used to compare differences in survival between groups. GraphPad Prism software (Version 7.0) was used to determine statistical significance among multiple studies. *P* values of less than 0.05 were considered significant. Statistical significance was denoted by $^{*}p < 0.05$, $^{**}p < 0.01$, or $^{***}p < 0.001$. The exact value of n, representing the number of mice in the experiments depicted, was indicated in the figure legends.